

Lone Higgs at the LHC

Ken Hsieh* and C.-P. Yuan†

Department of Physics and Astronomy,

Michigan State University, East Lansing, MI 48824, USA

(Dated: September 12, 2022)

Abstract

We address the possible scenario that the Large Hadron Collider (LHC) discovers only a Higgs boson after 10 fb^{-1} of operation, and attempt to identify this Higgs boson as that of the Standard Model (SM), the minimal universal extra dimension model (MUED), the littlest Higgs model with T -parity (LHT), or the minimal supersymmetric Standard Model (MSSM), using only the measurement of the product of gluon-fusion production cross section and the di-photon branching ratio. In MUED, by decoupling any new physics sufficiently to evade the discovery reach at the LHC, the deviation of the signal from the SM is not statistically significant. However, in LHT and MSSM, it is possible to have a significant deviation in the signal that is consistent with this "lone Higgs scenario", and, in the case of a very large suppression, we can distinguish MSSM and LHT before the discovery of any new resonances. Starting with the lone Higgs scenario and the deviation in this measurement from the Standard Model prediction (whether or not statistically significant), we offer tests that may discriminate the models and search strategies of discovering new physics signatures with increasing integrated luminosity.

*email: kensieh@pa.msu.edu

†email: yuan@pa.msu.edu

I. INTRODUCTION

The stability of the electroweak scale has driven the high energy physics community, both theorists and experimentalists alike, for nearly the past two decades. With the advent of the Large Hadron Collider (LHC), we can finally probe the mechanism of electroweak symmetry breaking (EWSB) and possibly new physics at the TeV scale that stabilizes the electroweak scale. However, as such new physics is still a mystery, we need to be prepared for all the possibilities. In addition, with the multitude of models of new physics and the possible associated experimental signatures, we are also faced with the ‘inverse problem’ of distinguishing models of new physics using the experimental data.

In this work, we investigate one of the possible scenarios at the LHC, and attempt to disentangle three generic models of new physics based on experimental measurements of a Higgs boson. We suppose that, after the first few years of operation with an integrated luminosity of 10 fb^{-1} , the LHC has only discovered a lone scalar boson with couplings to the W - and Z -bosons that are of the same magnitude as predicted in the Standard Model (SM). While discovering only a Higgs boson at the LHC (with an integrated luminosity of several 100 fb^{-1}) been dubbed a “Nightmare Scenario [1],” here we are only assuming no new physics, other than this Higgs boson, is seen at this stage of operation of the LHC, and leave open the possibility that new physics may be uncovered with further operation time. Indeed, one of the main goals of works of this type is to optimize further search strategies based on the information we have at hand from the discovered Higgs boson.

The main question that we attempt to answer in this work is: from the measurement of $B\sigma(gg \rightarrow h \rightarrow \gamma\gamma)$, which denotes the product the Higgs boson production cross section $\sigma(pp \rightarrow (gg \rightarrow h)X)$ and the di-photon decay branching ratio $\text{Br}(h \rightarrow \gamma\gamma)$, and its deviation from the SM prediction, can we identify this scalar boson as *the* Higgs boson in the SM, minimal universal extra dimensions (MUED), littlest Higgs with T -parity (LHT), or (the lightest CP -even boson in) the minimal supersymmetric standard model (MSSM)? If not, we investigate whether we can use this measurement as a hint or bias, and devise further search strategies of new physics based on its deviation from the SM, regardless whether such deviation is statistically significant. Questions of this type are in spirit similar to the LHC inverse problem [2], but with an emphasis on distinguishing the models rather than mapping

the regions of parameter spaces of a particular model from the data. While such LHC inverse problems have been studied in the literature, they attempt to distinguish models through properties, such as spin, of the new resonances discovered at the LHC. Our work here is also of similar spirit to Mantry et al. [3] [4] and Randall [5], where they discuss how the properties of the Higgs boson can be modified due to states that are not directly observable at the LHC.

Our work is organized as follows. In Section II, we discuss the precision to which the signal $B\sigma(gg \rightarrow h \rightarrow \gamma\gamma)$ can be measured at the LHC after 10 fb^{-1} of data. In Section III, we discuss the general pattern of deviations of the signal $B\sigma(gg \rightarrow h \rightarrow \gamma\gamma)$ in the parameter spaces of the models, and roughly map out regions in parameter spaces that such deviation can be significant. We also apply the results of LHC reaches in these models to map out regions of parameter spaces that can be consistent with the aforementioned lone Higgs scenario. In Section IV, we apply the lone Higgs scenario as constraints on the parameter spaces, and see how the signal is affected. In particular, we find that in the lone Higgs scenario with a large deviation in $B\sigma(gg \rightarrow h \rightarrow \gamma\gamma)$, we can potentially rule out MUED, and, in some cases, distinguish between the MSSM and LHT. Also in Section IV, we propose some parameter-independent tests that can also be used to distinguish these models. We conclude in Section V with a summary of our results and offer outlook for projects of this type.

II. A REVIEW OF HIGGS MEASUREMENTS AT THE LHC

In this section we present a brief overview of the detection of the Higgs boson and the measurement of its properties at the LHC. More details can be found at the ATLAS technical design report (TDR) [6] and CMS TDR [7], and references therein.

For reference, we show the production cross section of the Higgs boson via gluon-gluon fusion at the LHC $\sigma_h \equiv \sigma(pp \rightarrow (gg \rightarrow h^0)X)$ at the next-to-leading order in QCD, with the renormalization and factorization scales set to the mass of the Higgs boson (m_h), using the latest parton distribution functions (PDF), CTEQ 6.6M [8], in the top plot of Fig. 1. The uncertainties of this cross section, both the PDF-induced uncertainty as well as the relative difference with an earlier version of the PDF (CTEQ6.1), are of the order of a few percent

as shown in the lower plot of Fig. 1. The uncertainty in the luminosity will be on the order of 20% at the start of the LHC. However, the uncertainties in the measurements of the cross sections due to the uncertainty in the luminosity can be reduced partially by taking ratios of these cross sections to measured “standard candle” cross sections, such as $\sigma_{t\bar{t}} \equiv \sigma(pp \rightarrow t\bar{t}X)$ and $\sigma_Z \equiv \sigma(pp \rightarrow (Z^0 \rightarrow \ell^+\ell^-)X)$ [8].

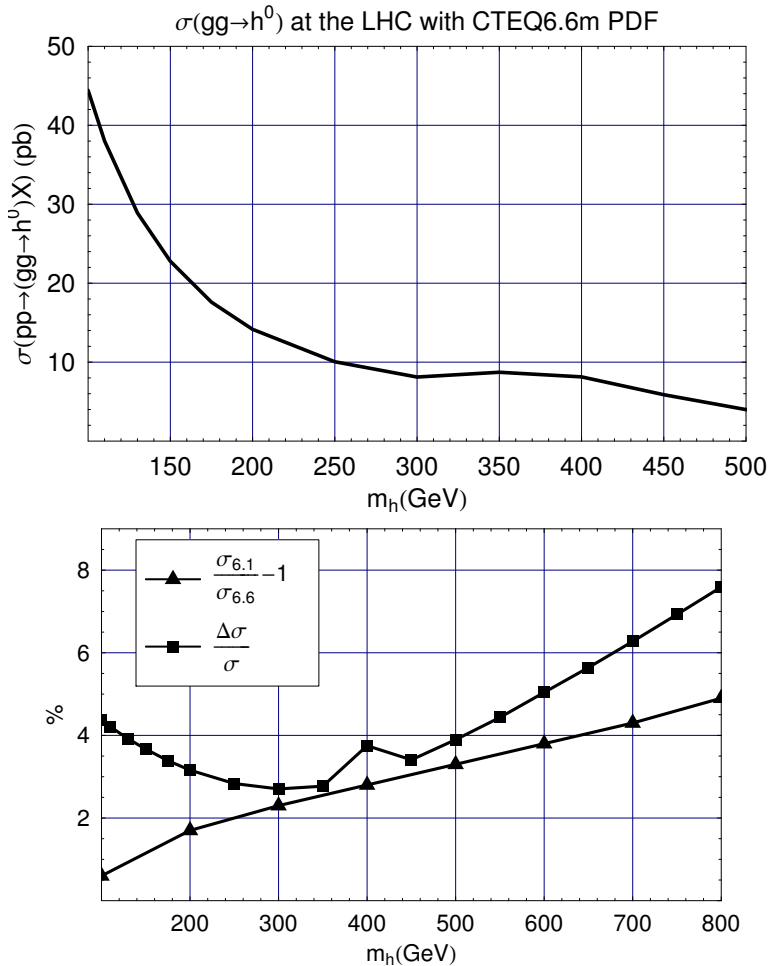


FIG. 1: The cross section σ_h at the LHC using the latest PDF, CTEQ6.6M [8] (top plot) and its PDF-induced uncertainty (bottom plot, boxed points) and relative difference with previous version of PDF, CTEQ6.1 (triangle points).

The detection channels of the Higgs boson depend significantly on its mass. Although the Higgs boson couples most strongly to the massive gauge bosons W^\pm, Z^0 and the top quark, for Higgs mass significantly lighter than the WW threshold ($m_h \lesssim 130$ GeV), the

decays $h \rightarrow WW, ZZ, \bar{t}t$ are kinematically inaccessible, and the dominant decay channel of the Higgs boson is $h \rightarrow \bar{b}b$. Unfortunately, the di-jet background at the LHC is expected to overwhelm this signal, and the most promising channel of detecting the Higgs boson is through its (loop suppressed) di-photon decay, $h \rightarrow \gamma\gamma$, with a branching ratio of about 0.2%. The di-photon channel offers a very clean signature of Higgs boson and enables a precise measurement of its mass. For $m_h > 130$ GeV, the decay channels $W^{(*)}W$ and $Z^{(*)}Z$, and (for even heavier m_h) $\bar{t}t$ become dominant. At the same time, the di-photon branching ratio decreases significantly.

As we are assuming that the discovered Higgs boson is (maybe only one of several Higgs bosons) responsible for electroweak symmetry breaking, the most general renormalizable operators involving this Higgs boson would be those in the SM. The loop contributions to these couplings from new physics will typically be of the percent level that are too small to be probed at the early stages of the LHC, and we may ignore the loop corrections to these couplings. On the other hand, the couplings a_{hgg} and $a_{h\gamma\gamma}$ of dimension-five di-gluon and di-photon operators that characterize the gluon-fusion production rate and di-photon width of the Higgs boson

$$a_{hgg} \frac{h}{v_{\text{ew}}} G_{\mu\nu}^A G^{A\mu\nu}, \quad a_{h\gamma\gamma} \frac{h}{v_{\text{ew}}} F_{\mu\nu} F^{\mu\nu}, \quad (1)$$

are one-loop at leading order in the SM, and loop contributions from new physics may be competitive. Thus, to study this discovered boson in a bottom-up approach, we consider an effective Lagrangian that includes all the renormalizable gauge and Yukawa operators as in the SM, but with arbitrary coefficients, and only consider the leading-order effects of these operators. In addition, we include the two dimension-five operators with arbitrary coefficients that parameterizes the leading effects of the yet-undiscovered new physics on the Higgs boson, and the measurement of $B\sigma(gg \rightarrow h \rightarrow \gamma\gamma)$ essentially measures the product of a_{hgg}^2 (which is proportional to the production cross section σ_h) and the decay branching ratio $\text{Br}(h \rightarrow \gamma\gamma)$. As the di-photon branching ratio is only significant for $m_h \lesssim 130$ GeV, we will only consider a Higgs boson with a mass within this range.

Since the PDF-induced uncertainty is of the order of 5%, the precision to which these couplings can be measured depends crucially on the uncertainty in the luminosity at the LHC. The precision of which the couplings in our effective Lagrangian can be measured at

the LHC has been extensively studied [9] [10]. From Zeppenfeld et al. [9], we see that with 100 fb^{-1} from both ATLAS [6] and CMS [7], the cross section $B\sigma(gg \rightarrow h \rightarrow \gamma\gamma)$ can be measured to about 10%. This uncertainty is defined as

$$\frac{\sqrt{N_S + S_B}}{N_S}, \quad (2)$$

where $N_S(N_B)$ is the number of signal (background) events. We refer the readers to the reference for the numbers of events, backgrounds, and the significance of the signal.

With only 10 fb^{-1} of data, we naively scale our error by a factor of $\sqrt{0.1}/0.1 \sim 3$, and use 30% as the accuracy to which $B\sigma(gg \rightarrow h \rightarrow \gamma\gamma)$ can be measured. Thus, the measurement of $B\sigma(gg \rightarrow h \rightarrow \gamma\gamma)$ with 10 fb^{-1} at LHC can only distinguish models of new physics from the SM only if it deviates by more than 30% from the SM prediction, and we will see that this can often places stringent constraints on the parameter spaces of new physics models, independent of the lone Higgs scenario.

III. MODELS OF NEW PHYSICS AND LONE HIGGS SCENARIOS

A. Minimal Supersymmetric Standard Model

1. $B\sigma(gg \rightarrow h \rightarrow \gamma\gamma)$ in MSSM

The minimal supersymmetric Standard Model (MSSM) is the most widely-studied model of new physics both in theory and experiment [11]. It extends the SM with superpartners that differ in spin by $1/2$ from their SM counterparts, and the electroweak scale is stabilized by the presence of these superpartners if they have masses of about 1 TeV. It is remarkable that in the MSSM the lightest CP -even boson has a mass that is bounded by about 125 GeV if the MSSM is to solve the hierarchy problem. As decay to WW^* and ZZ^* pairs are now kinematically suppressed, the di-photon channel is now the golden channel to search for the lightest CP -even Higgs boson.

Unfortunately, the MSSM comes with 105 parameters [11] and it is impossible to scan through such vast parameter space. We will make some simplifying assumptions that the first two generations of sfermions have mass matrices that are diagonal at the weak scale and the phases of all SUSY-breaking contributions are zero. These assumptions are consistent with

the various flavor-changing experimental constraints, and leave us with a reduced parameter space. With this reduced parameter space, the signal $B\sigma(gg \rightarrow h \rightarrow \gamma\gamma)$ can still vary greatly. For example, in Fig. 2, we use `hdecay` [12] (which includes the `FeynHiggs` package [13]) to show the deviation of $B\sigma(gg \rightarrow h \rightarrow \gamma\gamma)$ from the SM values for various values of M_A (the mass of the CP -odd Higgs boson in the MSSM), scanning over the s-top sector parameters

$$\begin{aligned} 300 \text{ GeV} &\leq M_{\tilde{Q}_3}, M_{\tilde{U}_3} \leq 1.5 \text{ TeV}, \\ -4\sqrt{M_{\tilde{Q}_3}M_{\tilde{U}_3}} &\leq A_t \leq 4\sqrt{M_{\tilde{Q}_3}M_{\tilde{U}_3}}, \end{aligned}$$

where $M_{\tilde{Q}_3}$ and $M_{\tilde{U}_3}$ are respectively the SUSY-breaking masses of the left- and right-handed s-tops (the superpartners the top quark), and $y_t A_t$ (where y_t is the top Yukawa coupling) is the coefficient of the trilinear interaction $\tilde{Q}_3 H_u^0 \tilde{U}_3$. We note the following points regarding the parameters in the s-top sector (also see Fig. 3).

- The scanned range of A_t includes the regions that give the largest mass for the lightest, CP -even Higgs boson, which occurs for $A_t^2 \sim 6M_{\tilde{Q}_3}M_{\tilde{U}_3}$. While $A_t^2 \sim 6M_{\tilde{Q}_3}M_{\tilde{U}_3}$ leads a large Higgs mass, the mixing in the s-top sector is $m_t(A_t - \mu \cot \beta)$, so we can have a large Higgs mass without having a light s-top with $M_{\tilde{Q}_3}, M_{\tilde{U}_3} \gg m_t$.
- To avoid s-tops with negative squared-mass, A_t must satisfy (for large $\tan \beta$)

$$A_t^2 < \frac{(M_{\tilde{Q}_3}^2 + m_t^2)(M_{\tilde{U}_3}^2 + m_t^2)}{m_t^2}. \quad (3)$$

For small $M_{\tilde{Q}_3}$ and $M_{\tilde{U}_3}$, it may not be possible to scan in the full region between $A_t \sim \pm 4(M_{\tilde{Q}_3}M_{\tilde{U}_3})^{1/2}$. For small $M_{\tilde{Q}_3}$ and $M_{\tilde{U}_3}$, our scanned range in A_t is limited requiring having two s-tops with positive masses.

- With large $M_{\tilde{Q}_3}$ and $M_{\tilde{U}_3}$, even though positive s-top masses may allow A_t^2 to be large relative to $M_{\tilde{Q}_3}M_{\tilde{U}_3}$, large A_t can lead to a negative squared mass for the lightest, CP -even Higgs boson. This occurs when we have

$$\frac{3y_t^4 v_{\text{ew}}^2}{2\pi^2} \left(\frac{1}{12} \frac{A_t^4}{M_{\tilde{Q}_3}^2 M_{\tilde{U}_3}^2} - \frac{A_t^2}{M_{\tilde{Q}_3} M_{\tilde{U}_3}} \right) \gtrsim M_Z^2 + \frac{3y_t^4 v_{\text{ew}}^2}{2\pi^2} \ln \frac{M_{\tilde{Q}_3} M_{\tilde{U}_3}}{m_t^2}, \quad (4)$$

where $v_{\text{ew}} (= 246 \text{ GeV})$ is the electroweak scale (i.e. the vacuum expectation value), and our scanned range of A_t does not include such large A_t .

For simplicity, we hold all other parameters fixed as

$$\begin{aligned}
M_{\tilde{\ell}} &= 100 \text{ GeV}, \\
M_{\tilde{w}} &= \mu = 200 \text{ GeV}, \\
M_{\tilde{g}} &= M_{\tilde{Q}} = 500 \text{ GeV},
\end{aligned}
\tag{5}$$

where $M_{\tilde{\ell}}(M_{\tilde{Q}})$ is any slepton (first two generations squark) soft mass, $M_{\tilde{g}}$ the gluino mass, $M_{\tilde{w}}$ the wino mass, and μ the chargino mass. The bino mass $M_{\tilde{b}}$ is determined assuming unified gaugino mass at the grand unification scale $M_{\text{GUT}} \sim 10^{16}$ GeV.

Though there is a general trend of suppression in $B\sigma(gg \rightarrow h \rightarrow \gamma\gamma)$ in Fig. 2, we see that the specific amount of suppression fluctuates with the parameters in the s-top sector as well as M_A . (We discuss the region where $B\sigma(gg \rightarrow h \rightarrow \gamma\gamma)$ is enhanced in the lower-right plot of Fig. 2 at the end of this subsection.) However, as we eventually will be interested in the lone Higgs scenario, the s-fermions and the gauginos should be heavy enough to evade discovery. In particular, having large s-top masses and large $A_t^2 (\sim 6M_{\tilde{Q}_3} M_{\tilde{U}_3})$ leads to a large Higgs mass in addition to heavy s-top masses to evade discovery.

In Fig. 2, we see that, as m_h increases, the fluctuation in $B\sigma(gg \rightarrow h \rightarrow \gamma\gamma)$ decreases, signaling the decoupling of the s-top sector. We show this more explicitly in Fig. 4 where we scan over A_t in the range of $\pm 3(M_{\tilde{Q}_3} M_{\tilde{U}_3})^{1/2}$ holding $M_{\tilde{Q}_3}$ and $M_{\tilde{U}_3}$ fixed. We also fix other parameters as Eq. (5), and fix $\tan\beta = 10$ and $M_A = 1$ TeV. With $M_{\tilde{Q}_3}$ and $M_{\tilde{U}_3}$ fixed as 1 TeV (2 TeV), the fractional deviation in $B\sigma(gg \rightarrow h \rightarrow \gamma\gamma)$ changes by 11% (3%) as we scan over A_t . The plot shows that with larger $M_{\tilde{Q}_3, \tilde{U}_3}$, the deviation in $B\sigma(gg \rightarrow h \rightarrow \gamma\gamma)$ is less sensitive to the variation in A_t as both the s-tops decouple. We therefore consider a limited lone Higgs scenario where the s-top soft masses are large enough that, in addition to evade direct discovery at the LHC, the s-top contributions to the gluon-gluon fusion and diphoton decay amplitudes decouple regardless of the value of A_t . As the s-top contributions decouple, we attribute the suppression in $B\sigma(gg \rightarrow h \rightarrow \gamma\gamma)$ to M_A and $\tan\beta$ in this limited lone Higgs scenario.

In this work we will restrict our attention to the range $10 < \tan\beta < 30$, where both the top and bottom Yukawa couplings are perturbative and there is no danger for light or negative s-tau or s-bottom masses from $\tan\beta$ -enhanced mixing when $\mu m_{b(\tau)} \tan\beta \sim M_{\tilde{b}(\tilde{\tau})}^2$, where \tilde{b} and $\tilde{\tau}$ are respectively the s-bottom and s-tau.

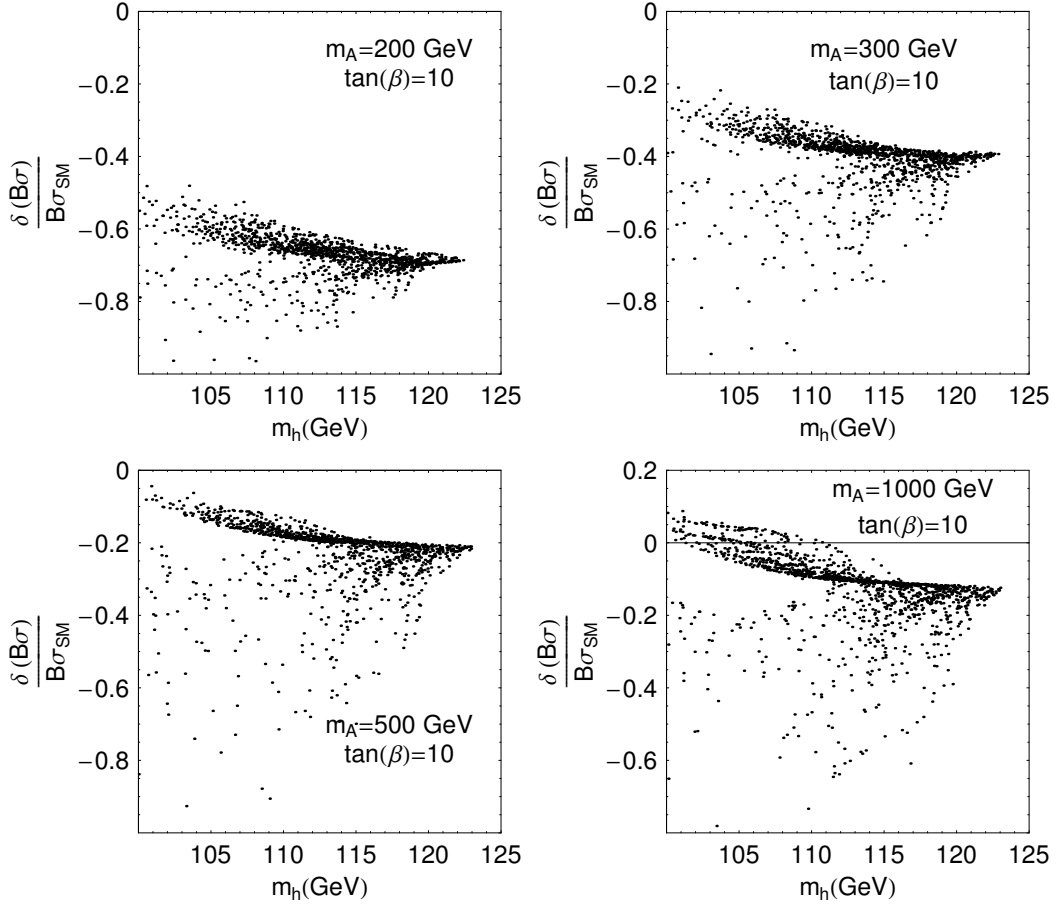


FIG. 2: The fractional deviation of $B\sigma(gg \rightarrow h \rightarrow \gamma\gamma)$ as a function of Higgs mass in MSSM for various values of $M_A=200$ (top left), 300 (top right), 500 (bottom left), and 1000 (bottom right) GeV. The s-top soft masses $M_{\tilde{Q}_3}$ and $M_{\tilde{U}_3}$ are scanned from 300 GeV to 1.5 TeV, with A_t scanned in the range of $\pm 4(M_{\tilde{Q}_3} M_{\tilde{U}_3})^{1/2}$. The other SUSY-breaking values are fixed as $M_{\tilde{\ell}} = 100$ GeV, $M_{\tilde{w}} = \mu = 200$ GeV, and $M_{\tilde{g}} = M_{\tilde{Q}} = 500$ GeV.

To study the effects of M_A and $\tan\beta$ in $B\sigma(gg \rightarrow h \rightarrow \gamma\gamma)$ in the decoupling limit of heavy sfermions and gauginos, in Fig. 5 we show the dependence in $B\sigma(gg \rightarrow h \rightarrow \gamma\gamma)$ as a

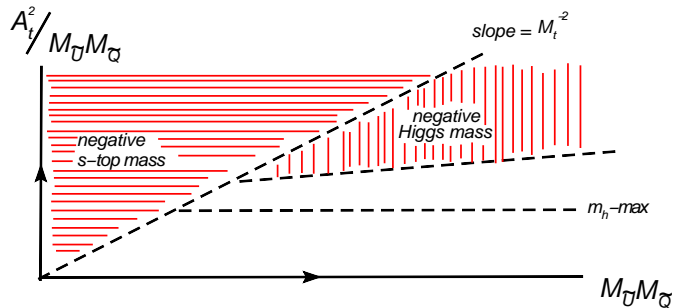


FIG. 3: The schematic plot of allowed parameter space in the s-top sector. This plot is not drawn to scale. The line denoted as $m_h\text{-max}$ denotes the line with $A_t^2/M_{\tilde{Q}_3}M_{\tilde{U}_3} = 6$, and the mass of the lightest, CP -even Higgs boson is maximized at 1-loop. Having too large A_t can lead to a negative s-top mass (horizontally hashed region). However, even if A_t is not large enough to lead to a negative s-top mass, it can be large enough to lead to a negative mass for the lightest, CP -even Higgs boson (vertically hashed region).

function of M_A for $\tan\beta = 10, 20$, and 30 , with other parameters fixed as

$$\mu = M_2 = M_{\tilde{\ell}} = 1 \text{ TeV}, \quad (6)$$

$$M_{\tilde{g}} = M_{\tilde{Q}} = 2.5 \text{ TeV}, \quad (7)$$

$$A_t = 5 \text{ TeV}, \quad (8)$$

$$A_b = A_\tau = 0. \quad (9)$$

This set of parameters differs from those in Eq. 5 because we will eventually be interested in the MSSM lone Higgs scenarios. As we will see in the next subsection, these parameters give sufficiently heavy sfermions and gauginos that are out of the reach at the LHC with 10 fb^{-1} of integrated luminosity. We note that the dependence in $\tan\beta$ on $B\sigma(gg \rightarrow h \rightarrow \gamma\gamma)$ is small in this range of $\tan\beta$. In particular, $B\sigma(gg \rightarrow h \rightarrow \gamma\gamma)$ can be suppressed by more than 30% for $M_A \lesssim 330 \text{ GeV}$. In the next subsection we will investigate whether this region can be consistent with a lone Higgs scenario given the expected LHC reach for the heavy Higgs bosons.

We conclude this subsection with a brief discussion of the possibility of having an enhancement in $B\sigma(gg \rightarrow h \rightarrow \gamma\gamma)$ in the MSSM. In the lower-right plot of Fig 2, in the region with small Higgs mass ($m_h \sim 100 \text{ GeV}$) we have enhanced $B\sigma(gg \rightarrow h \rightarrow \gamma\gamma)$ that is con-

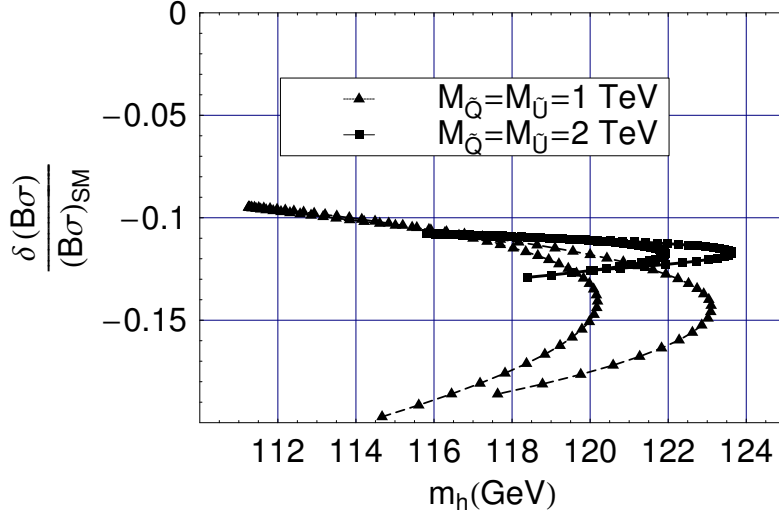


FIG. 4: The fractional deviation of $B\sigma(gg \rightarrow h \rightarrow \gamma\gamma)$ with A_t scanned over the range $\pm 3(M_{\tilde{Q}_3}M_{\tilde{U}_3})^{1/2}$ with $M_{\tilde{Q}_3} = M_{\tilde{U}_3} = 1$ TeV (triangle points), and $M_{\tilde{Q}_3} = M_{\tilde{U}_3} = 2$ TeV (square points). With larger $M_{\tilde{Q}_3, \tilde{U}_3}$, the deviation in $B\sigma(gg \rightarrow h \rightarrow \gamma\gamma)$ is less sensitive to the variations in A_t because the s-top sector decouples. Here we fix $\tan\beta = 10$ and $M_A = 1$ TeV in addition to those labelled in Eq. (5). For each set of s-top sector parameters, there are two arcs on the plot because positive values of A_t gives a larger Higgs mass than negative values of A_t at two-loop.

trary to the typical trend of suppression we note earlier. This is because the enhancement in the production $\sigma(gg \rightarrow h)$ (due to light-stops with small mixing) compensates for the small suppression in the branching ratio $\text{Br}(h \rightarrow \gamma\gamma)$ (due to large $M_A = 1$ TeV). On the other hand, in the lone Higgs scenario we consider here with two heavy s-tops, the production cross-section $\sigma(gg \rightarrow h)$ is only enhanced slightly relative to the SM [14], and the suppression in $B\sigma(gg \rightarrow h \rightarrow \gamma\gamma)$ is dominantly due to a suppression in $\text{Br}(h \rightarrow \gamma\gamma)$ resulting from $\tan\beta$ -enhanced $h\bar{b}b$ and $h\bar{\tau}\tau$ couplings, leading to a larger total decay width of the Higgs boson. (We also note that it is possible to have a suppression in the production cross-section $\sigma(gg \rightarrow h)$ in the MSSM, leading to a so-called gluo-phobic Higgs, when there is a large hierarchy between the s-tops $m_{t_2}^2 \gg m_{t_1}^2$ and a significant mixing in the s-top sector [14].)

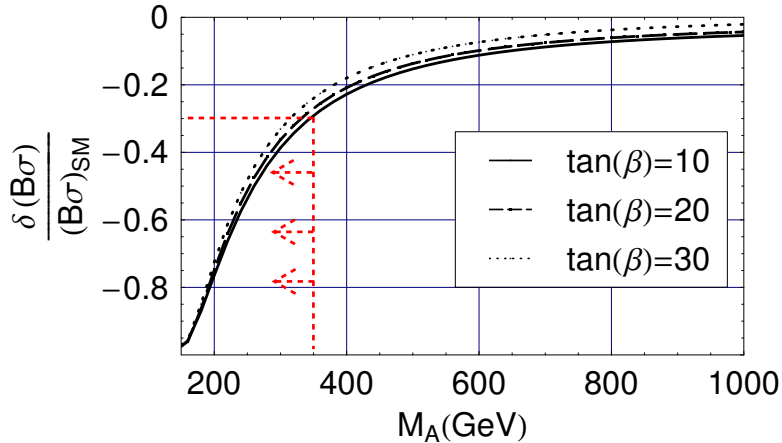


FIG. 5: The fractional deviation of $B\sigma(gg \rightarrow h \rightarrow \gamma\gamma)$ as a function of M_A for $\tan\beta = 10, 20$, and 30. The soft masses are fixed to evade LHC discovery as $\mu = M_{\tilde{w}} = M_{\tilde{\ell}} = 1$ TeV, $M_{\tilde{g}} = M_{\tilde{Q}} = 2.5$ TeV, $A_t = 5$ TeV, and $A_b = A_\tau = 0$. For $M_A < 330$ GeV, there is significant deviation in $B\sigma(gg \rightarrow h \rightarrow \gamma\gamma)$ from the SM.

2. Lone Higgs Scenario in the MSSM

To investigate the viable lone Higgs scenarios in the MSSM, we here briefly summarize the known results in the literature regarding the LHC reach of the MSSM particles. The summary of MSSM discovery potential at the CMS experiment at the LHC for the constrained MSSM (CMSSM) is shown in the CMS TDR [7], and we include it in Fig. 6. We here focus on reaches of several experimental signatures that allow us to place general bounds on the MSSM parameter space, and we will simplify the MSSM parameter space in terms of four general types of resonances in addition to the Higgs boson. These four types are: (i) colored superpartners (gluino and squarks), (ii) sleptons, (iii) neutralinos and charginos, and (iv) heavy Higgs bosons. We discuss the discovery reach of each in turn.

a. Gluino and squarks

In the CMSSM parameterization of the MSSM parameters by the set $\{m_0, m_{1/2}, A_0, \tan\beta, \text{sgn}(\mu)\}$, the colored superpartners are generically heavier than the non-colored superpartners, and the search for SUSY involves tracking down the cascade decays of pair-produced squarks and/or gluinos. While the nature of the cascades depends

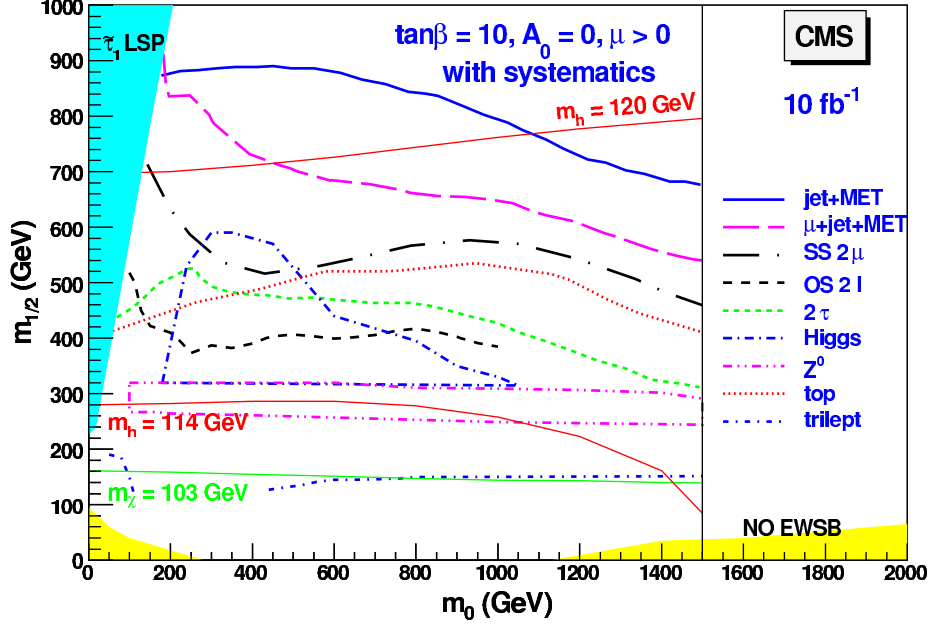


FIG. 6: This figure is taken from the CMS TDR [7], and summarizes the MSSM reach on m_0 - $m_{1/2}$ plane at CMS with an integrated luminosity of 10 fb^{-1} , except for the Higgs search, which assumes 2 fb^{-1} .

on the details of the MSSM spectra (see CMS TDR [7] for the various possibilities), the initial step of the cascade always involves emitting at least a quark and all cascades always end with the stable, lightest superpartner (LSP) that leaves the detector as missing energy (assuming that R -parity is conserved). Thus, the signature of jets plus missing energy provides the best reach of the MSSM space (line labelled 'jet+MET' in Fig. 6), and the reach is roughly $m_{1/2} \sim 900 \text{ GeV}$, corresponding to a gluino mass of $M_{\tilde{g}} \sim 2.7m_{1/2} \sim 2.4 \text{ TeV}$. We also note that this reach is only mildly dependent on m_0 , and the squark masses are less constrained by this reach. Nevertheless, we make a reasonable simplifying assumption that the reach for squarks is also $M_{\tilde{Q}} \sim 2.4 \text{ TeV}$.

b. Sleptons

Moving away from the CMSSM parameterization, if a large hierarchy existed between the colored superpartners and the non-colored superpartners such that at the LHC the gluino and squarks can not be directly produced at the LHC, then SUSY searches involve the production channels of non-colored superpartners, such as chargino-neutralino associated

production and slepton pair-productions. While the right-handed slepton (superpartner of the right-handed lepton) can only decay to the LSP directly in CMSSM, the left-handed slepton can decay to $\chi_{1,2}^0$ and χ_1^\pm if kinematically allowed (depending on $m_{1/2}$). In both cases of direct slepton pair production and indirect slepton production (through the decays of neutralinos and charginos from associated chargino-neutralino associated production), there are always at least two leptons from the decays of the sleptons. Furthermore, in the case of direct slepton pair-production, the two leptons must have opposite sign. The signature of the direct slepton pair production and indirect production then involves two leptons, missing energy, and jet veto, and the exclusion plot in the reference is reproduced in Fig. 7 (see Chapter 13, Section 15 of the CMS TDR [7] for details on the cuts and significance of the reach). For large $\tan\beta$, the largest slepton mass is roughly $m_{\tilde{l}}^2 \sim m_0^2 + (0.5)m_{1/2}^2 + 0.27M_Z^2$, and using $m_0 = m_{1/2} = 150$ GeV from Fig. 7, we obtain $m_{\tilde{l}} \sim 200$ GeV. For further references, there are detailed studies of slepton searches in the literature [15][16][17].

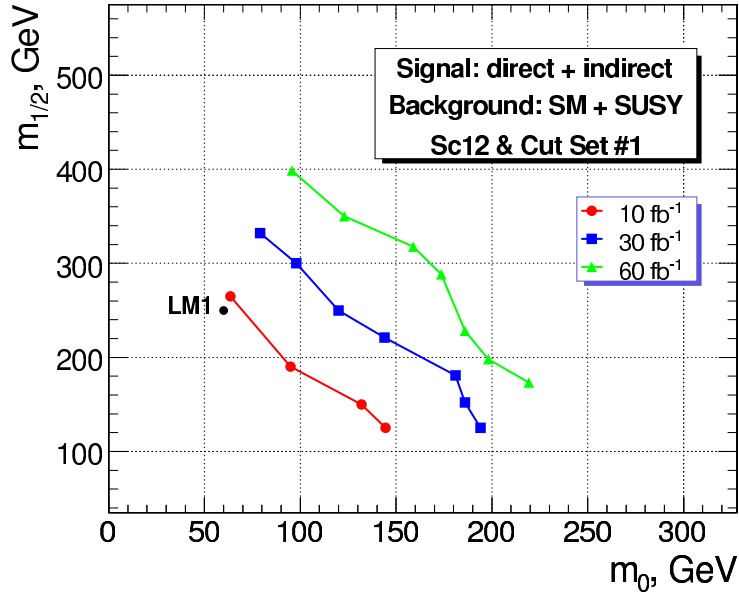


FIG. 7: This plot is taken from CMS TDR [7] and shows CMS reach of pair production of slepton on m_0 - $m_{1/2}$ plane with $\tan\beta = 10$, $A_0 = 0$, and the sign μ is positive. The experimental signatures of the events are two leptons, missing energy, and no jets.

c. Neutralinos and charginos

The reach of neutralino(χ_i^0)/chargino(χ_i^\pm) sector involves a tri-lepton signature that arises

from $pp \rightarrow \chi_2^0 \chi_1^\pm X$ with $\chi_2^0 \rightarrow \ell^+ \ell_- \chi_1^0$ (through a slepton $\tilde{\ell}$, which may be real or virtual) and $\chi_1^\pm \rightarrow \chi_1^0 W^{(*)\pm} \rightarrow \chi_1^0 \ell^\pm \nu_\ell$. The lepton pair from the decay of χ_2^0 will be of the same flavor, opposite sign (SFOS), while the lepton from χ_1^\pm can be any flavor. In addition to the three leptons and missing energy, no jets participate in this process and a jet veto can be used (see Chapter 13, Section 14 of the CMS TDR [7] for details), and the reach is presented in the bottom blue curve in Fig. 6 denoted as “trilept”. As with the case of the gluino/squark reach, we see that the curve is only mildly dependent on m_0 and has a value of $m_{1/2} \sim 150$ GeV for $m_0 > 400$ GeV, and $m_{1/2}$ fluctuates between 100 GeV and 200 GeV for $m_0 < 400$ GeV. The wino (bino) mass is related to m_0 in CMSSM by $M_2 \sim 0.8m_{1/2}$ ($M_1 \sim 0.4m_{1/2}$). Thus, taking the conservative reach of $m_{1/2} \sim 200$ GeV gives $M_2 \sim 160$ GeV and $M_1 \sim 80$ GeV. To obtain the full spectra in the neutralino/chargino sector requires the knowledge of the Higgsino mass μ . However, assuming that $\mu > M_2$ and that μ is not nearly degenerate with M_2 , we do not expect large mixing in the neutralino/chargino sector, and we can approximate $M_{1,2}$ as the masses of $M_{\chi_{1,2}^0}$.

d. Higgs bosons

Because the variation in $B\sigma(gg \rightarrow h \rightarrow \gamma\gamma)$ in the MSSM has strong dependence on M_A in the decoupling limit of heavy s-fermions and gauginos, the LHC reaches of the heavy Higgs bosons play important roles in the determination of whether we have a lone Higgs scenario with a large deviation in $B\sigma(gg \rightarrow h \rightarrow \gamma\gamma)$. The reach of the MSSM heavy Higgs bosons has been studied in the literature [6][7][18], and we have taken figures from these references in Figs. 8 and 9.

Although in this work we focus on the lone Higgs scenario with 10 fb^{-1} of LHC data, we could only find discovery reach for the heavy Higgs bosons with 30 fb^{-1} of data. We will assume that the reach of the MSSM heavy Higgs bosons are further with 30 fb^{-1} of data than with 10 fb^{-1} , and conservatively apply the discovery reach of the heavy MSSM Higgs bosons at 30 fb^{-1} to our 10 fb^{-1} lone Higgs scenario.

The discovery reach of the charged Higgs bosons H^\pm is presented Fig. 8, with $pp \rightarrow tbH$, where H^\pm is either produced through the decay of a top quark $t \rightarrow H^+ b$ produced in $t\bar{t}$ production if $M_{H^\pm} < m_t$, or, if $M_{H^\pm} > m_t$, produced through a virtual b^* via $b^* \rightarrow tH^-$ in a $\bar{b}b$ production. The charged Higgs boson then decays via $H^- \rightarrow \tau\bar{\nu}_\tau$, and as the coupling of $H^+\bar{t}b$ is $\tan\beta$ -enhanced, stronger bounds can be placed with larger $\tan\beta$. However, for

$\tan\beta \lesssim 30$, the reach on M_A is less than $M_A = 200$ GeV with CMS, while ATLAS does not set a bound on M_A for $4 \leq \tan\beta \leq 25$. Thus, the discovery reach for the charged Higgs bosons does not impose a severe constraint on M_A .

The discovery reaches of the neutral Higgs bosons h, H , and A at CMS and ATLAS are presented Fig. 9 using various processes as indicated on the plots. As with the charged Higgs, these searches depend on $\tan\beta$ -enhanced couplings. For a given value of M_A , these heavy Higgs boson discovery reaches limit the lone Higgs scenario with an upper bound on $\tan\beta$. The strongest discovery reach for the neutral Higgs boson comes from the ATLAS search involving $H/A \rightarrow \bar{\tau}\tau$ as shown in Fig. 9(c), which places an upper bound of $\tan\beta < 15$ if we are to have $M_A < 330$ GeV in a lone Higgs scenario. For larger values of $\tan\beta$, we would need larger values of M_A to have viable lone Higgs scenarios, and it is difficult to distinguish the lone Higgs scenario from the SM by the suppression in $B\sigma(gg \rightarrow h \rightarrow \gamma\gamma)$. With 300 fb^{-1} of integrated luminosity, the LHC can also discover the A if $\tan\beta$ is small ($1 \leq \tan\beta \leq 2$), as shown in Fig. 9(c), through the process $gg \rightarrow A \rightarrow \bar{\tau}\tau$, whose rate is significantly larger than that of the SM Higgs boson $gg \rightarrow h \rightarrow \bar{\tau}\tau$. As the bounds from ATLAS are more stringent, we will mainly use Fig. 9(c) to set bounds on the lone Higgs scenario in the MSSM in the next section. (For details, see the ATLAS TDR[6], the CMS TDR [7], Gennai et al. [18], and reference therein.)

e. Possibilities of a Lone Higgs Scenario in MSSM

TABLE I: Summary of LHC reach for different types of superpartners of the MSSM with 10 fb^{-1} of integrated luminosity. The reach of the heavy Higgs bosons involve 30 fb^{-1} of integrated luminosity. The assumptions we make are in parenthesis.

Superpartner	LHC reach	Signature used
Gluino/squarks	$M_{\tilde{g}} \sim 2.5 \text{ TeV}$ ($M_{\tilde{q}} \sim 2.5 \text{ TeV}$)	Jets and missing energy
Sleptons	$M_{\tilde{l}} \sim 200 \text{ GeV}$	OS leptons, missing energy, and jet veto
Neutralinos/charginos	$M_2 \sim 160 \text{ GeV}$ ($\mu > M_2$)	Tri-lepton, missing energy, and jet veto
Heavy Higgs bosons	$M_A \sim 230(480) \text{ GeV}$ ($\tan\beta = 10(20)$)	$\phi \rightarrow \tau^+\tau^-, \tau \rightarrow (jj, ej, \mu j)$

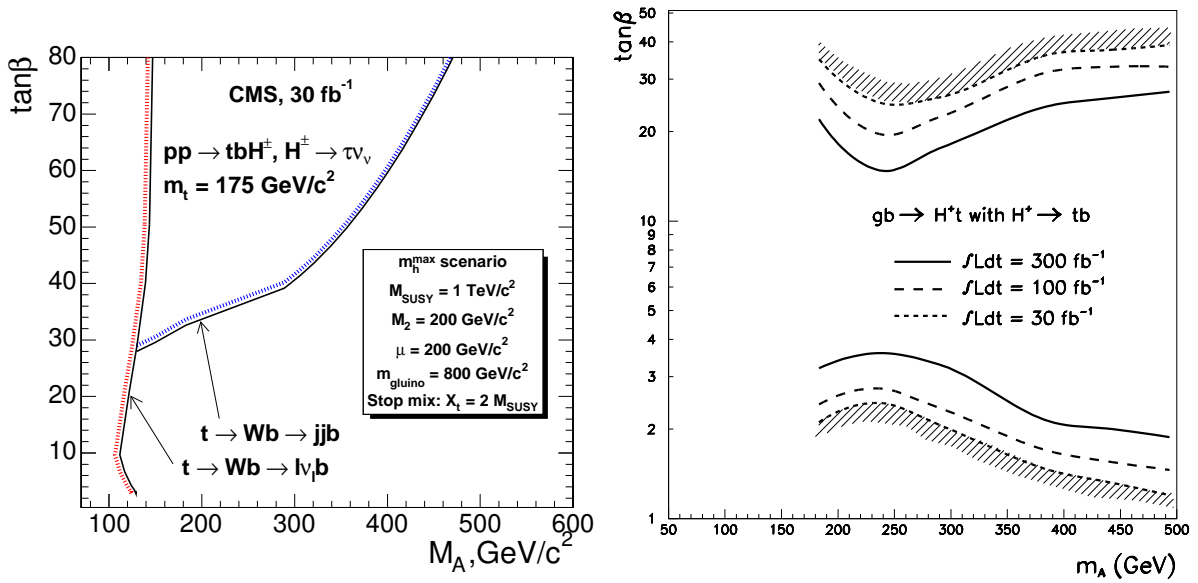


FIG. 8: The left plot is taken from the CMS TDR [7], and the right plot taken from the ATLAS TDR [6]. These plots summarize the LHC reach of heavy charged Higgs bosons at the CMS (left) and ATLAS (right) using channels as indicated on the plots.

The LHC reach for the four types of superpartners is summarized in Table I. To obtain a consistent lone Higgs scenario with the MSSM, we simply require the superpartners to be heavier than the discovery reach at the LHC. On the other hand, we see from Figs. 2 and 5 that the signal $B\sigma(gg \rightarrow h \rightarrow \gamma\gamma)$ is most sensitive to M_A . With all s-fermions and gauginos out of reach at 10 fb^{-1} , having a large deviation in $B\sigma(gg \rightarrow h \rightarrow \gamma\gamma)$ requires $M_A < 330 \text{ GeV}$ (see Fig. 5), which is only consistent with a lone Higgs scenario for $\tan\beta \lesssim 15$ from Fig. 9(c).

This is a very strong constraint: with our self-imposed range of $10 < \tan\beta < 30$, with 10 fb^{-1} of LHC data, if we have only discovered a Higgs boson whose deviation in $B\sigma(gg \rightarrow h \rightarrow \gamma\gamma)$ is suppressed by more than 30% relative to the SM, then it can be consistent with the MSSM only if $M_A < 330 \text{ GeV}$ and $\tan\beta < 15$. Furthermore, given $\tan\beta (M_A)$ we can set more stringent bounds on M_A ($\tan\beta$) using the upper-right plot in Fig. 9(c). Suppose we know that $\tan\beta = 10$ from, for example, the branching ratio of $h \rightarrow \bar{\tau}\tau$, the upper bound on M_A is $M_A < 230 \text{ GeV}$ because any lower value of M_A would give rise to additional resonances at the LHC.

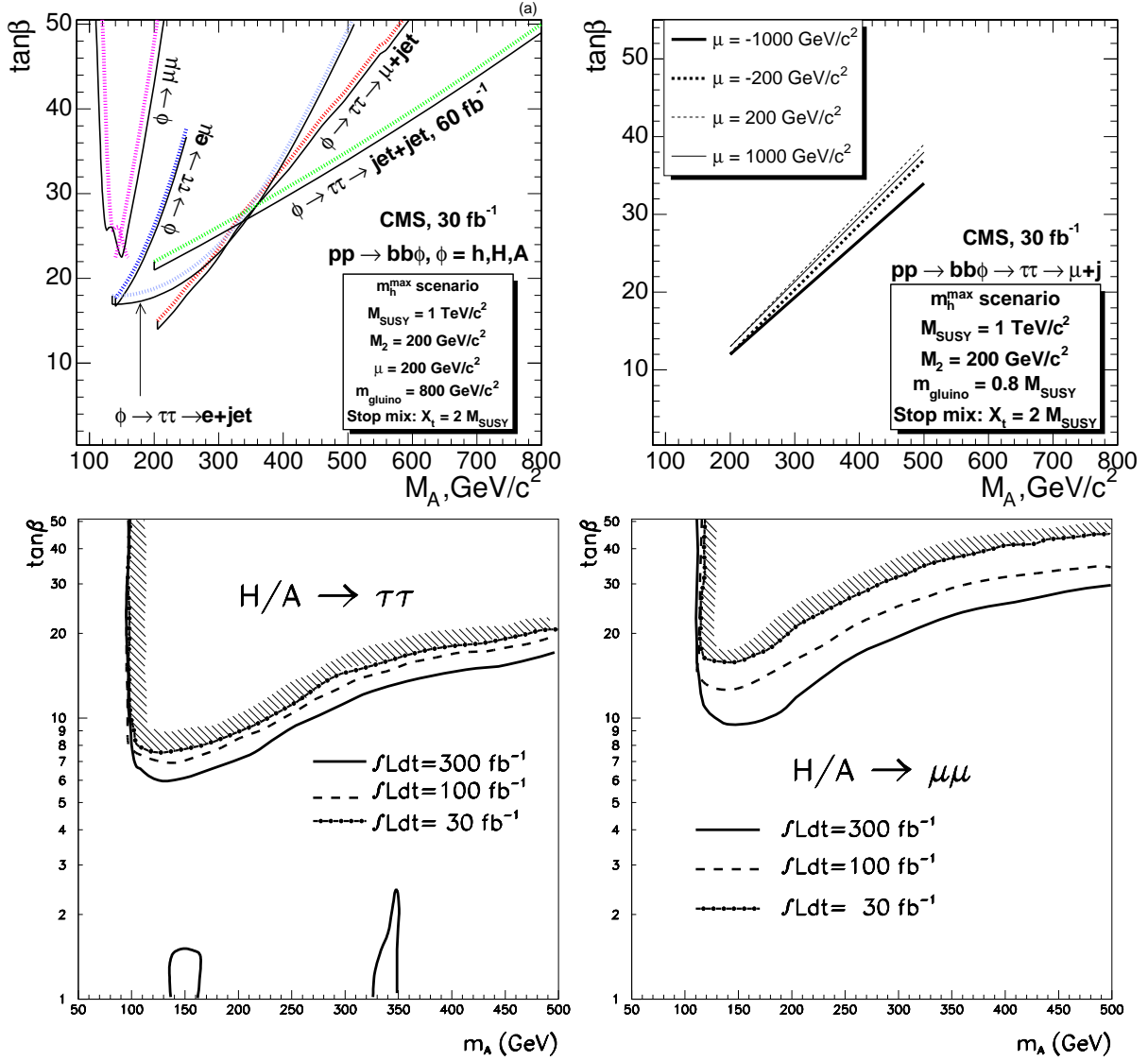


FIG. 9: Fig. 9(a) is taken from the CMS TDR [7], Fig. 9(b) from Gennai et al. [18], and Figs. 9(c) and (d) from ATLAS TDR [6]. These plots summarize the CMS and ATLAS reach of heavy neutral Higgs bosons in various channels, as indicated on the plots. Fig. 9(c) sets the strongest constraints on having a lone Higgs scenario with large deviations in $B\sigma(gg \rightarrow h \rightarrow \gamma\gamma)$.

We can further constrain viable MSSM lone Higgs scenarios with a large deviation in $B\sigma(gg \rightarrow h \rightarrow \gamma\gamma)$ from the measured value of the branching ratio $\text{Br}(b \rightarrow s\gamma)$ with 1σ uncertainty [19]

$$\text{Br}(b \rightarrow s\gamma)_{\text{exp}} = (355 \pm 26) \times 10^{-6}, \quad (10)$$

if we assume minimal flavor violation (MFV) scenario. A rigorous definition of MFV can be found in D’Ambrosio [20]. In the MSSM we can have MFV with universal soft s-fermion masses and having the trilinear couplings proportional to the Yukawa couplings at an arbitrary energy scale, which we pick to be near the weak scale. In Fig. 10, we plot $\text{Br}(b \rightarrow s\gamma)$ using `SusyBsg` [21] (with the aid of `SOFYSUSY` [22]) as a function of M_A for $\tan\beta = 10$ and $\tan\beta = 15$, holding all other parameters fixed as in Eq. (9). With these parameters, the s-fermions, charginos, and neutralinos are all heavy enough to evade discovery at the LHC with 10 fb^{-1} . From Fig. 10, for $\tan\beta = 10$ (15), we must have $M_A > 420 \text{ GeV}$ (380 GeV) to be consistent with $\text{Br}(b \rightarrow s\gamma)$ within 1σ uncertainties, and this excludes a lone Higgs scenario with a large suppression compared to the SM prediction since such lone Higgs scenario requires $M_A < 350 \text{ GeV}$ (see Fig. 5). On the other hand, to be consistent with $\text{Br}(b \rightarrow s\gamma)$ within 3σ uncertainties, for $\tan\beta = 10$ (15), the limits on M_A relaxes to $M_A > 260 \text{ GeV}$ (240 GeV), and we can have lone Higgs scenarios with large suppressions in $B\sigma(gg \rightarrow h \rightarrow \gamma\gamma)$ compared to the SM prediction. If the LHC discovers a lone Higgs scenario with a suppression in $B\sigma(gg \rightarrow h \rightarrow \gamma\gamma)$ of more than 55% from the SM, then Fig. 5 implies that $M_A < 240 \text{ GeV}$, which is not consistent with the measurement of $\text{Br}(b \rightarrow s\gamma)$ assuming MFV. In this case, if the MSSM is to explain the observed suppression, the flavor structures in the MSSM must deviate from those given by MFV. Since we are interested mainly in constraints on lone Higgs scenarios from direct searches and the assumption of MFV imposes very stringent constraints, we do not assume MFV in our current work.

As we will show a later subsection, the LHT model can also give rise to a lone Higgs scenario with a large suppression in $B\sigma(gg \rightarrow h \rightarrow \gamma\gamma)$ relative to the SM, and we will investigate how we may distinguish between these two models in Section IV.

B. Littlest Higgs model with T -parity

1. $B\sigma(gg \rightarrow h \rightarrow \gamma\gamma)$ in LHT

In Littlest Higgs model with T -parity [23][24][25][26], based on little Higgs models [27][28][29][30], the SM Higgs doublet is a pseudo Nambu-Goldstone boson (NGB) of two independent spontaneously broken symmetries at a scale Λ . The collective symmetry breaking mechanism of generating the Higgs mass ensures that its quadratic divergence vanish

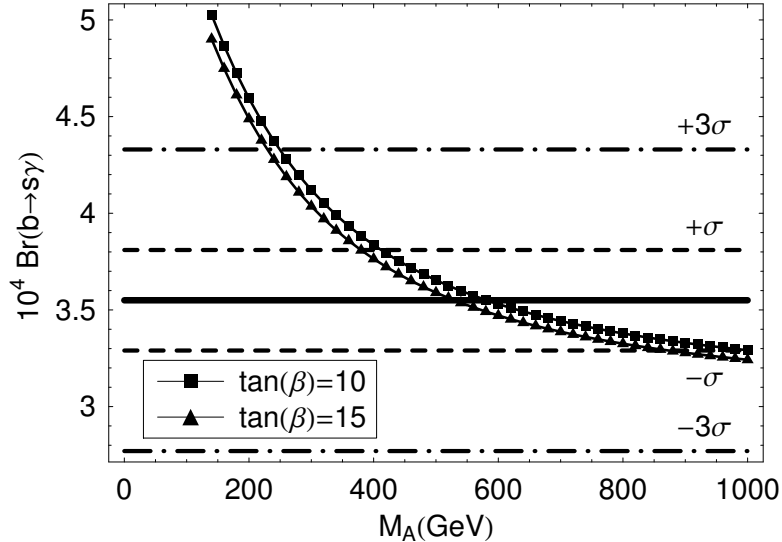


FIG. 10: The branching ratio $\text{Br}(b \rightarrow s\gamma)$ as a function of M_A for $\tan\beta = 10$ and $\tan\beta = 15$. The other parameters are fixed as in Eq. (9) to evade the discovery of the s-fermions, the charginos, and the neutralinos. The horizontal lines indicate current experimental value (solid), 1σ uncertainties (dashed), and 3σ uncertainties (dot-dashed).

at one-loop level, and the electroweak scale can be stabilized with $\Lambda \sim 10$ TeV. The contributions to electroweak precision observables are loop-suppressed with the introduction of a T -parity. Most of the new states that are accessible at the LHC must be pair-produced because they are odd under T -parity while all the SM particles are even under T -parity. The mass scale of these T -odd particles is of the order $f \sim (4\pi)^{-1}\Lambda$, and the lower bound on f from electroweak precision tests is about 500 GeV [31].

The Higgs production and di-photon branching ratio in LHT has been studied in Chen et al. [32]. As noted in the reference, the gluon-fusion production cross section in LHT is always suppressed relative to the Standard Model. The reference also points out that the gluon fusion process $gg \rightarrow h$ is only dependent on f , and independent the parameters of the extended top sector because changes in the masses of the top-partners are compensated by changes in the $h\bar{T}_+T_+$ coupling, where T_+ is the T -even top partner. The di-photon branching ratio of the Higgs boson, however, can be enhanced even though the di-photon width is smaller than that of SM. In the left (right) plot in Fig. 11, we show the deviation

in $B\sigma(gg \rightarrow h \rightarrow \gamma\gamma)$ from the SM values for several values of f (m_h) as a function of m_h (f). The decay channel $h \rightarrow A_- A_-$ is allowed when $m_h > 2M_{A_-}$, and for low values of $f = 500$ GeV, this gives a sharp drop in the suppression of $B\sigma(gg \rightarrow h \rightarrow \gamma\gamma)$ relative to the SM around $m_h \sim 150$ GeV. We first note that, similar to the case of heavy s-fermions and gauginos in the MSSM, the signal is always suppressed relative to the SM, and this may give us two interpretations of a lone Higgs scenario with a large suppression in $B\sigma(gg \rightarrow h \rightarrow \gamma\gamma)$. We also note that, from Fig. 11, for $m_h < 120$ GeV, the signal deviates less than 30% from the SM, and may not be distinguished from the SM.

To have large deviation in $B\sigma(gg \rightarrow h \rightarrow \gamma\gamma)$ in LHT, we then need both $m_h > 120$ GeV as well as a low value of f . For example, with $m_h = 130$ GeV, the signal only deviates more than 30% from the SM for $f < 560$ GeV. To investigate whether this is consistent with the lone Higgs scenario, we have to first summarize the discovery potential of the various new resonances in LHT, which we turn to next.

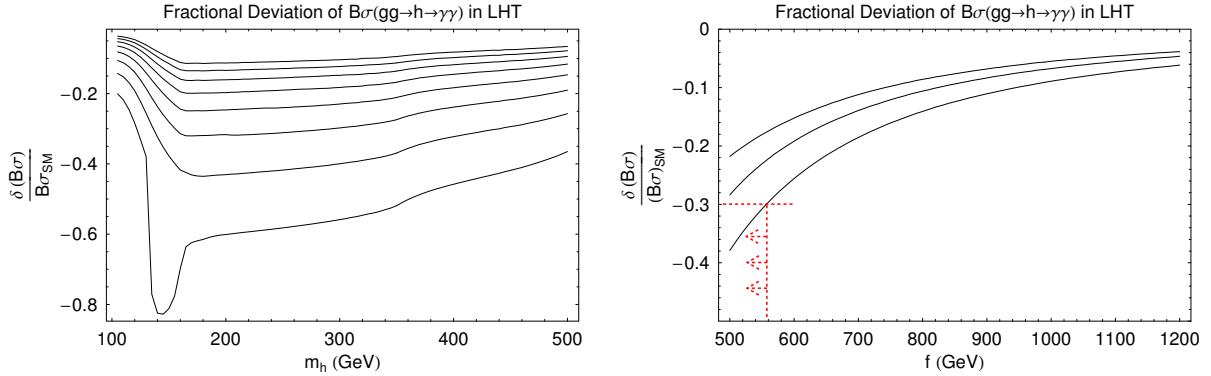


FIG. 11: The plot on the left shows the fractional deviation of $B\sigma(gg \rightarrow h \rightarrow \gamma\gamma)$ as a function of Higgs mass in LHT for various values of $f = (500, 600, 700, 800, 900, 1000, 1100, 1200)$ GeV. The lowest curve on the plot (showing the most deviation from the SM) correspond to $f = 500$ GeV. The plot on the right shows the fractional deviation of $B\sigma(gg \rightarrow h \rightarrow \gamma\gamma)$ as a function of f mass in LHT for $m_h = 110$ (top curve), 120 (middle), and 130 (bottom) GeV. For $f < 560$ GeV, the suppression is greater than 30%, and significantly different from the SM.

2. Lone Higgs Scenario in LHT

The discovery reaches for the T -odd particles have been studied in the literature, and we discuss in turn the three classes of new resonances of LHT that can potentially be seen at the LHC: (i) T -odd gauge bosons (W_H^\pm and A_H), (ii) T -odd quarks (Q_-) and leptons (L_-) that are T -partners to the SM quark and leptons of the first two generations, and, (iii) T -odd and T -even top quarks (T_\pm).

a. T -odd gauge bosons

The LHC phenomenology of the T -odd gauge bosons has been studied by Cao et al. [33], and the discovery reach of its results are presented in Fig. 12. While the masses of the T -odd gauge bosons are determined by f alone ($M_{W_H} = M_{Z_H} = gf \sim 0.64f$ and $M_{A_H} = g'(\sqrt{5})^{-1}f \sim 0.16f$), the masses of the T -odd fermions for the first and second generations involve additional inputs κ_q and κ_ℓ , and are related to f by $M_{(Q_-, L_-)} \sim \sqrt{2}\kappa_{(q,\ell)}f$. The production of T -odd gauge bosons $\bar{q}q \rightarrow W_H^+W_H^-$ is dominated by s -channel exchange in Z^* and the t -channel exchange in Q_-^* interferes destructively with the Z^* -exchange diagram. By raising κ_q , the Q_- -exchange amplitude becomes smaller, and the production cross section is enhanced, leading to a stronger reach for W_H^\pm .

The search strategies for discovering W_H depends crucially on whether the channels $W_H^\pm \rightarrow \ell L_-, qQ_-$ are kinematically accessible, and as such depends on κ_q and κ_ℓ . Assuming $\kappa_q > 1$ and $\kappa_\ell = 0.5$ so that $W_H \rightarrow WA_H$ is the only decay channel of W_H , the signal of pair-production of W_HW_H then includes the leptonic decays of W and missing energy because A_H is stable. From the top two plots of Fig. 12, with 10 fb^{-1} at the LHC, the 5σ discovery reach of W_H is possible only if $\kappa_q > 2$ for $f \sim 500 \text{ GeV}$ and extends to $f \sim 650 \text{ GeV}$ for $\kappa_q \sim 4$. For smaller values of κ_q , 3σ discovery is possible for $\kappa_q \sim 1$.

On the other hand, assuming that $\kappa_\ell = 0.3$ so that the cascade $W_H \rightarrow \ell L_- \rightarrow \ell \ell' A_H$ (with one of ℓ and ℓ' being a neutrino) is now allowed. While the signature of W_HW_H pair production now still contains two leptons and missing energy, the transverse momenta of the leptons are now typically higher (for the same M_{W_H}) and the SM background can be reduced more efficiently with the same cut on the lepton transverse momentum (see Cao et al. [33] for details). The results of this search are shown in the lower two plots of Fig. 12, which clearly indicates a further reach than the top two plots (with $\kappa_\ell = 0.5$) of the same

figure. With $\kappa_\ell = 0.3$ and 10 fb^{-1} of data, the LHC can now discover W_H for $f < 750 \text{ GeV}$ with $\kappa_q = 0.5$ at 5σ level. With $\kappa_q = 2.0$ and 10 fb^{-1} of data, the reach for W_H extends to $f < 1.1 \text{ TeV}$.

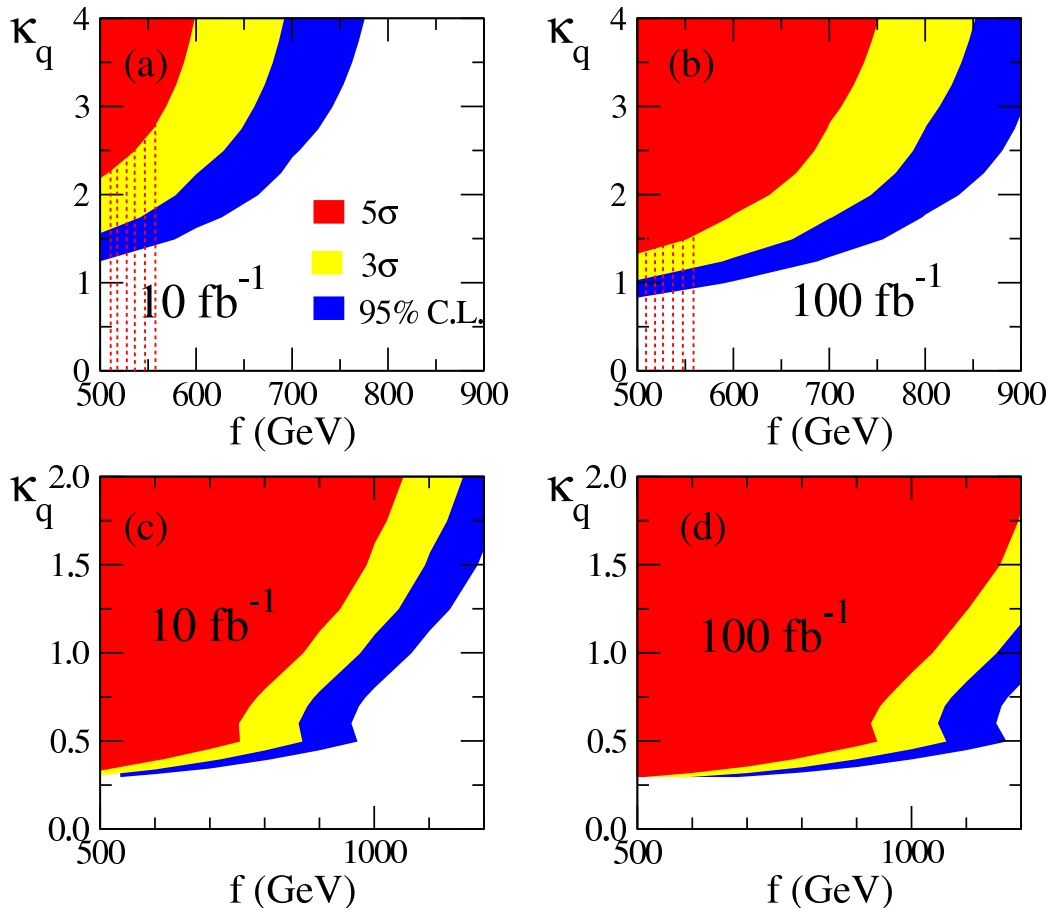


FIG. 12: These plots are taken from Cao et al. [33] and present the discovery contours of T -odd gauge bosons in on κ_q - f plane. The top two plots have $\kappa_\ell = 0.5$, so that $W_H \rightarrow WA_H$ is the only allowed decay channel at tree-level. The lower two plots have $\kappa_\ell = 0.3$, so W_H dominantly decays through the cascade $W_H \rightarrow L_\ell \rightarrow A_H \ell \ell$. For the case of $\kappa_\ell = 0.5$, we have hashed with vertical lines the regions viable with a lone Higgs scenario for a large deviation in $B\sigma(gg \rightarrow h \rightarrow \gamma\gamma)$.

b. T -odd quarks and leptons

The Tevatron and LHC phenomenology of T -odd fermions has been studied in the literature [34][35] [36]. The T -odd fermions will be pair-produced at the LHC and decay

through a cascade (if kinematically allowed) to A_H or decay to A_H directly, and the missing energy from A_H may fake the MSSM signatures [34]. The cascade decay of Q_- via $Q_- \rightarrow qW_H \rightarrow qWA_H$ is possible as long as $\kappa_q > g(\sqrt{2})^{-1} \sim 0.46$. Assuming universal and flavor-diagonal κ_q for both the up and down types of quarks, the 5σ discovery contours of Q_- for various integrated luminosities are presented on $\kappa-f$ plane in Choudhury et al. [36], which we show in Fig. 13 and briefly summarize the results below.

The cascade decays of pair-produced \bar{Q}_-Q_- can have the structure $\bar{Q}_-Q_- \rightarrow qqW_H^+W_H^- \rightarrow qqW^+W^-A_HW_H$, and leptonic decays of both W gives a signature of two jets, two opposite-sign leptons, and missing energy. One can also replace one W_H in the cascade by Z_H , which decays via $Z_H \rightarrow A_H(h \rightarrow \bar{b}b)$. The signature now contains one single lepton, $\bar{b}b$ pair from Higgs decay, two jets, and missing energy.

In Fig. 13, for a given f , we can evade the discovery of Q_- with a large enough κ (heavy enough Q_-). Furthermore, the reach of f decreases as κ increases; for example, with 10 fb^{-1} , the reach on f decreases from 950 GeV to 500 GeV as κ increases from 0.6 to 1.6. Beyond $\kappa > 1.6$, with 10 fb^{-1} , the reach of f is less than 500 GeV, which is excluded by electroweak precision tests.

It is interesting to note that we need large κ_q to evade discovery of Q_- , while we need small κ_q to evade the discovery of W_H , and we will explore this further later in this work. For now, we simply note that for $f = 560 \text{ GeV}$, $\kappa > 1.3$ is required to evade discovery of Q_- at 10 fb^{-1} .

c. Top partners

In addition to the top quark, the particle content in the top sector of LHT includes two top-partners T_\pm with opposite T -parity. The spectrum in the top sector is determined by the two parameters $\lambda_{1,2}$ in addition to f , with masses given by $m_t \simeq \lambda_1\lambda_2(\sqrt{\lambda_1^2 + \lambda_2^2})^{-1}v_{\text{ew}}$, $m_{T_+} \simeq (\sqrt{\lambda_1^2 + \lambda_2^2})f$, and $m_{T_-} \simeq \lambda_2f$, so that T_- is always lighter than T_+ . The collider signatures of T_- have been investigated in by Matsumoto et al. [37], the LHC reach of the T -odd top quark is about 900 GeV with 50 fb^{-1} [37]. On the other hand, this does not translate to a bound on f that we seek for since one can always make both top-partners heavy by making λ_2 large, and adjust λ_1 to accommodate the top quark mass (at the expense of fine-tuning).

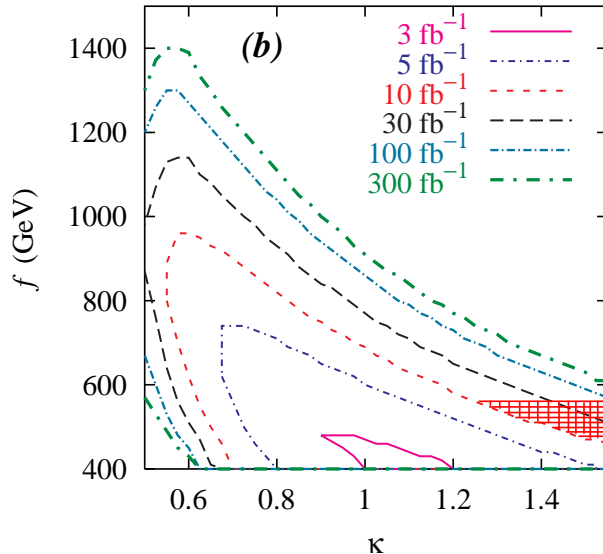


FIG. 13: This plot is taken from Choudhury et al. [36] and presents the discovery contours of T -odd fermions in on κ - f plane, where $\kappa_q = \kappa_\ell = \kappa$ is assumed universal and flavor-diagonal for the first two generations. We have hashed out (in red) the region of having a viable lone Higgs scenario with large suppression in $B\sigma(gg \rightarrow h \rightarrow \gamma\gamma)$ ($f < 560$ GeV).

d. Summary

To find out whether LHT with large deviation in $B\sigma(gg \rightarrow h \rightarrow \gamma\gamma)$ ($f < 560$ GeV and $m_h \sim 130$ GeV) is consistent with a lone Higgs scenario, we combine the results of the previous subsections. We note from Fig. 13 that the discovery potential of the T -odd fermions with 10 fb^{-1} limits a universal κ to be either $\kappa < 0.55$ or $\kappa > 1.3$. We discard the region $\kappa < 0.55$ with $f \sim 500$ GeV from our considerations for lone Higgs scenario because this region contains a rather light Q_- with a mass of about 400 GeV, which was shown to be difficult to detect at the LHC. With such light Q_- , although the process considered in Choudhury et al. [36] ($pp \rightarrow Q_- \bar{Q}_- \rightarrow q\bar{q}W_H^\pm Z_H \rightarrow bb + jj + \ell^\pm + \cancel{E}_T$) can not yield results that significant enough to claim discovery, we suspect other optimized searches dedicated to this region of parameter space may discover Q_- , and this particular region of parameter space may warrant further study.

We start our search for a lone Higgs scenario with $\kappa_\ell = 0.5$, so that W_- only decays to $W_- \rightarrow WA_-$, and the viable region in the $\kappa_q - f$ plane is shown in Fig. 12(a). On the other hand, discovery reach for the T -odd quarks indicates the viable region as shown in

Fig. 13. For $f = 560$ GeV, the lone Higgs scenario constraints $1.25 < \kappa_q < 3$ from the 5σ discovery potentials of W_- ($\kappa_q < 3$) and Q_- ($1.25 < \kappa_q$). Thus, there is a consistent lone Higgs scenario with large deviations in $B\sigma(gg \rightarrow h \rightarrow \gamma\gamma)$ in LHT, and we will discuss the phenomenology of the lone Higgs scenario in the next section.

C. Minimal Universal Extra Dimension

1. $B\sigma(gg \rightarrow h \rightarrow \gamma\gamma)$ in MUED

The Universal Extra Dimension (UED) model [38] extends the spacetime with one additional spatial, flat dimension that is accessible to all fields of the SM (hence the name universal) [39][40][41][42]. This extra dimension is compactified on a circle with radius R and orbifolded with a Z_2 symmetry. The SM particles are zeroth Kaluza-Klein (KK) modes, and the higher KK modes have tree-level masses roughly nR^{-1} , where n is the KK number. However, the masses of the KK modes are renormalized by interactions localized at the orbifold fixed points [43]. These effects are scale-dependent and are thus generated by renormalization effects. In Minimal UED (MUED) [44], an ansatz is made about the values of these boundary interactions at the cutoff scale, and the model is parameterized by two free parameters: R and the cutoff scale Λ .

In MUED, a KK-parity is conserved such that the lightest KK-odd particle (LKP) is stable and can serve as dark matter. In the particular case of MUED, the lightest KK-odd particle is a mixture of (dominantly) the first KK modes of the hypercharge gauge boson $B_\mu^{(1)}$ and (sub-dominantly) the neutral $SU(2)$ gauge boson $W_{3\mu}^{(1)}$ [45][46][47][48][49]. The Wilkinson Microwave Anisotropy Probe (WMAP) observations [50] of the dark matter relic density translates into a tight constraint on R^{-1} of $500 \text{ GeV} < R^{-1} < 600 \text{ GeV}$, and this range of R^{-1} in MUED implies colored KK modes with sub-TeV masses, so that they are accessible at the LHC.

Some typical spectra of MUED can be found in Cheng et al. [44], and a review of the collider signatures of generic UED models is presented by Hooper et al. [51]. Here we simply reproduce formula for the masses of the KK particles relevant to our discussion with the MUED ansatz in Cheng et al. [44]. We are interested in the mass of the KK W^\pm -boson and the two KK top quarks (corresponding to KK modes of the left- and right-handed

components of the SM top quark) because they contribute to the di-photon decay of the Higgs boson, and the KK top quarks also contribute to the gluon-fusion production of the Higgs boson, We are also interested in the mass of the KK gluon as we will use it to analyze the LHC discovery reach on the parameter R^{-1} . The masses of the n^{th} KK gluon and KK W^{\pm} -boson are given by

$$m_{g^{(n)}}^2 = n^2 R^{-2} \left(1 + \frac{23}{2} \frac{g_3^2}{16\pi^2} \ln \frac{\Lambda^2}{\mu^2} \right), \quad (11)$$

$$m_{W^{(n)}}^2 = n^2 R^{-2} \left(1 + \frac{15}{2} \frac{g^2}{16\pi^2} \ln \frac{\Lambda^2}{\mu^2} \right), \quad (12)$$

where g_3 is the strong coupling. At every non-zero KK level there are two KK top quarks with the mass matrix

$$\begin{pmatrix} nR^{-1} + \delta m_{Q_3^{(n)}} & m_t \\ m_t & -nR^{-1} - \delta m_{U_3^{(n)}} \end{pmatrix}, \quad (13)$$

where the radiative corrections are given by

$$\delta m_{Q_3^{(n)}} = nR^{-1} \left(3 \frac{g_3^2}{16\pi^2} + \frac{27}{16} \frac{g^2}{16\pi^2} + \frac{1}{16} \frac{g'^2}{16\pi^2} - \frac{3}{4} \frac{y_t^2}{16\pi^2} \right) \ln \frac{\Lambda^2}{\mu^2}, \quad (14)$$

$$\delta m_{U_3^{(n)}} = nR^{-1} \left(3 \frac{g_3^2}{16\pi^2} + \frac{g'^2}{16\pi^2} - \frac{3}{2} \frac{y_t^2}{16\pi^2} \right) \ln \frac{\Lambda^2}{\mu^2}, \quad (15)$$

where g and g' are the electroweak gauge couplings. We choose the renormalization scale to be $\mu = R^{-1}$ and $\Lambda = 10R^{-1}$, so the masses of the first KK modes of the gluon and W -boson are approximately

$$m_{g^{(1)}} \simeq 1.23 R^{-1}, \quad (16)$$

$$m_{W^{(1)}} \simeq 1.05 R^{-1}. \quad (17)$$

For the first KK modes of the top quark, having $\mu = R^{-1}$ and $\Lambda = 10R^{-1}$ gives us the mass matrix

$$\begin{pmatrix} 1.13 R^{-1} & m_t \\ m_t & -1.09 R^{-1} \end{pmatrix}, \quad (18)$$

and when $R^{-1} \gg m_t$, the mass eigenvalues can be approximately by the diagonal entries

$$m_{t_2^{(1)}} \simeq 1.13 R^{-1}, \quad (19)$$

$$m_{t_1^{(1)}} \simeq 1.09 R^{-1}. \quad (20)$$

In MUED, the strengths of the gauge and Yukawa interactions of the Higgs boson are the same as those in the SM. However, its effective di-gluon and di-photon couplings differ significantly from those in the SM because of the additional contributions induced by the KK partners of the top quark and the W -bosons. The effects of these KK modes have been computed by Petriello [52], and it is found that the presence of KK top quarks always enhances the production rate of Higgs boson via gluon-gluon fusion. We adapt the results of this reference to `hdecay` [12], taking into account the radiative corrections to the masses of the KK top quarks. (Including the radiative corrections, however, does not qualitatively modify the conclusions of Petriello [52].)

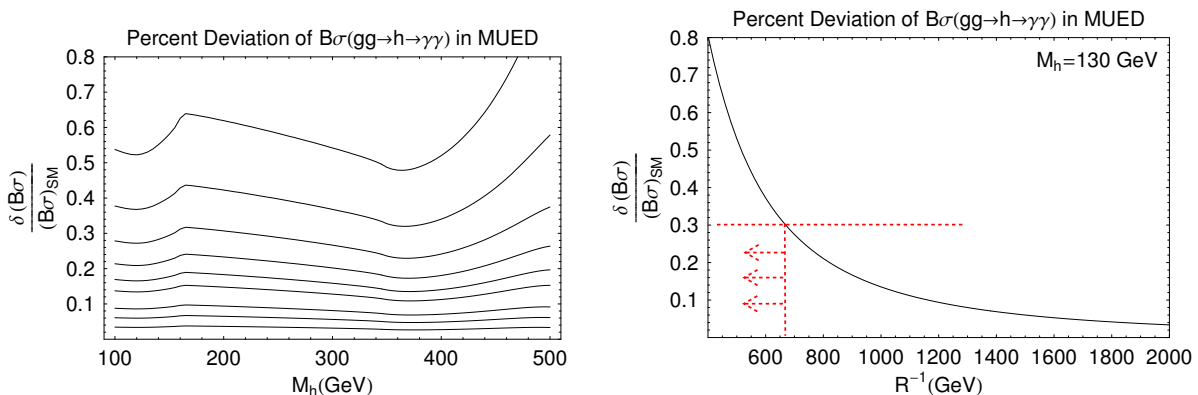


FIG. 14: The plot on the left shows the fractional deviation of $B\sigma(gg \rightarrow h \rightarrow \gamma\gamma)$ as a function of Higgs mass in MUED for various values of R^{-1} . From top to bottom, the values of R^{-1} (in GeV) are respectively 500, 600, 700, 800, 900, 1000, 1250, 1500, and 2000. In each case, we choose $\Lambda = 10R^{-1}$, and sum over the contributions from the lowest 10 KK levels. The plot on the right shows the fractional deviation of $B\sigma(gg \rightarrow h \rightarrow \gamma\gamma)$ as a function of R^{-1} in MUED for $m_h = 130$ GeV, and only for $R^{-1} < 650$ GeV is there a large enhancement in $B\sigma(gg \rightarrow h \rightarrow \gamma\gamma)$.

In the left plot of Fig. 14, we show the deviation signal $B\sigma(gg \rightarrow h \rightarrow \gamma\gamma)$ from the SM values for several values of R^{-1} as a function of the Higgs mass. We first note that for $500 \text{ GeV} < R^{-1} < 600 \text{ GeV}$ the product $B\sigma(gg \rightarrow h \rightarrow \gamma\gamma)$ is at least 35% (and at most 70%) above the SM results for Higgs mass in the range of $100 \text{ GeV} < m_h < 200 \text{ GeV}$. Together with the accessibility of the KK top quarks and KK gluons (with masses on the order of 700 GeV) at the LHC, this scenario can be distinguished from the SM. Furthermore, for $R^{-1} > 700 \text{ GeV}$, the signal enhancement is less than 30%, and it would be difficult to

distinguish the signal from the SM. In this case, the UED model may still explain dark matter with mass spectra that deviate from the MUED ansatz, and R^{-1} in Fig. 14 should be interpreted as the mass scale of the KK top quarks and gauge bosons through Eqs. (17) and (20).

Since the di-photon branching ratio is significant only if the Higgs boson is significantly lighter than the WW threshold, we focus on a light Higgs boson with $m_h \lesssim 130$ GeV. From Fig. 14, we also see that the deviation of the signal is roughly independent of Higgs mass in the range of $100 \text{ GeV} < m_h < 140 \text{ GeV}$, and we plot the deviation in signal $B\sigma(gg \rightarrow h \rightarrow \gamma\gamma)$ from the SM values as a function of R^{-1} in the second plot of Fig. 14 for $m_h = 130$ GeV, where we also see that for $R^{-1} > 700$ GeV, the deviation of the signal is less than 30%. Thus, the viable region in the MUED model for producing sizeable ($> 30\%$) enhancement in $B\sigma(gg \rightarrow h \rightarrow \gamma\gamma)$ as compared to SM is $R^{-1} \lesssim 700$ GeV, and we turn to a discussion about the discovery reach of the various KK resonances at the LHC to see if this region of R^{-1} can be consistent with a lone Higgs scenario.

2. Lone Higgs Scenario in the MUED

Qualitatively, the particle content and interactions of the MUED model is similar to MSSM in many ways in that each particle in the SM is extended with a partner. Instead of superpartners with spins that differ by half integer in MSSM, the MUED has KK modes with the same spin. The role of R -parity in the MSSM is played by K -parity in the MUED. In addition to giving rise to a dark matter candidate, such parity ensures that these partners must be pair-produced at the LHC.

Assuming that the colored KK states are heavier than the non-colored KK states (as is the case in the MUED ansatz), we would expect the LHC collider signatures of the KK gluons and quarks to follow similar paths as those of the gluino and squarks of the MSSM. The KK gluons/quarks would be pair-produced and decay through a cascade that ends with the LKP. As with the case of the MSSM, the signature would again be jets with missing energy, and we can reasonably approximate the discovery reach of the KK gluon and quarks to be the same as the gluino and the squark of the MSSM, which is 2.4 TeV for the mass of the gluino. For discovery reach of the KK quarks, we make the same simplifying assumption

that we made for the discovery reach of the squarks of the MSSM and assume that the reach for the KK quarks is also 2.4 TeV.

Since $R^{-1} \sim 700$ GeV corresponds to a KK gluon with a mass of approximately 860 GeV (see Eq. (17)), the KK gluon is within the reach of LHC using MSSM gluino discovery potential as a guide. We therefore do not have a consistent lone Higgs scenario with $R < 700$ GeV. To see what types of lone Higgs scenarios can be consistent with the MUED spectra, we note that once R^{-1} is large enough so that we enter the lone Higgs scenario ($M_g^{(1)} \gtrsim 2.4$ TeV so that $R^{-1} \gtrsim 1.95$ TeV via Eq. (17)), the signal $B\sigma(gg \rightarrow h \rightarrow \gamma\gamma)$ is enhanced only by 5% (see Fig. 14), which is well below the expected sensitivity of the LHC, even with 100 fb⁻¹ of data. This result should be contrasted with MSSM, where decoupling the s-top and gauginos still allowed a large suppression in $B\sigma(gg \rightarrow h \rightarrow \gamma\gamma)$. As stated earlier, in the MSSM this suppression comes from $\tan\beta$ -enhanced decay widths $\Gamma(h \rightarrow \bar{b}b)$ and $\Gamma(h \rightarrow \bar{\tau}\tau)$, and thus a suppression in the branching ratio $\text{Br}(h \rightarrow \gamma\gamma)$. In MUED, the couplings of the Higgs boson to the SM fermions are the same as those in the SM, and the deviation in $B\sigma(gg \rightarrow h \rightarrow \gamma\gamma)$ comes only from the KK top quarks and gauge bosons contributions, which decouples accordingly as $R^{-1} \rightarrow \infty$.

The MUED ansatz with $R^{-1} \gtrsim 1.95$ TeV also means that the KK leptons and gauge bosons are out of the reach at the LHC, since the masses of all these particles are of the order R^{-1} . Once we move away from the MUED ansatz, however, the KK states can in principle have independent masses and the discovery reach of the KK states do not translate to bounds on R^{-1} without a more fundamental organizing principle. Since in this work we study the signal $B\sigma(gg \rightarrow h \rightarrow \gamma\gamma)$ only using the MUED ansatz with Λ fixed as $\Lambda = 10R^{-1}$, without worrying about constraints and implications of the LKP as dark matter, we will simply report that a lone Higgs scenario is consistent with the MUED ansatz with $R^{-1} > 1.95$ TeV, with the reasonable assumption that the discovery reach of the KK gluon is the same as the gluino of the MSSM. However, in this case, the MUED new physics signal can not be easily distinguished from the SM. We will discuss how to distinguish the various models of new physics in the next section.

IV. DISTINGUISHING THE MODELS

A. Brief summary of results

TABLE II: The possibilities of new physics model based on the deviation of $B\sigma(gg \rightarrow h \rightarrow \gamma\gamma)$ from the SM, without imposing constraints of being consistent with a lone Higgs scenario.

	$m_h < 130$ GeV	$m_h > 130$ GeV
Enhanced	MUED	MUED
Similar	MSSM, MUED, LHT	LHT, MUED
Suppressed	MSSM, LHT	LHT

At this point, we summarize our findings so far. As noted earlier, it is useful to focus in the range of $m_h < 130$ GeV because the lightest CP-even Higgs can not be heavier than this bound in the MSSM, and, above this mass range the di-photon branching ratio drops, and it will be more useful to examine other modes of decay. First, we do not restrict ourselves to the lone Higgs scenario and include the possibilities that new physics is light and there can be significant deviations of the signal. In addition, from our analysis earlier, we also expect to see additional resonances when there is a significant deviation of $B\sigma(gg \rightarrow h \rightarrow \gamma\gamma)$ compared to the SM.

TABLE III: The possibilities of new physics model based on the deviation of $B\sigma(gg \rightarrow h \rightarrow \gamma\gamma)$ from the SM, imposing the conditions of being consistent with the lone Higgs scenario, i.e. that no new physics is seen at the LHC with 10 fb^{-1} of integrated luminosity and $m_h < 130$ GeV.

	$m_h < 130$ GeV
Enhanced	-
Similar	MSSM, MUED, LHT
Suppressed	MSSM, LHT

Stepping towards the lone Higgs scenario, we impose the conditions that the Higgs is lighter than 130 GeV and no additional new resonances has been directly seen at the LHC

after 10 fb^{-1} of operation. This is presented in Table III. As noted earlier, decoupling the KK tops and gauge bosons in MUED such that they are not directly accessible at the LHC after 10 fb^{-1} necessarily implies that the resulting Higgs boson would have a signal that is similar to the SM. In LHT with $m_h < 130 \text{ GeV}$, the deviation of $B\sigma(gg \rightarrow h \rightarrow \gamma\gamma)$ is only more than 30% for in the limited ranges of $f < 560 \text{ GeV}$ and $m_h \sim 130 \text{ GeV}$, and this region of parameter space is a viable lone Higgs scenario for $1.3 < \kappa_q < 3.0$. The MSSM can also lead to a viable lone Higgs scenario with large deviation in $B\sigma(gg \rightarrow h \rightarrow \gamma\gamma)$, for example, with $M_A = 300 \text{ GeV}$ and $\tan\beta = 10$.

Although we noted earlier that, relative to the SM, the signal $B\sigma(gg \rightarrow h \rightarrow \gamma\gamma)$ is always enhanced in MUED and suppressed in LHT, in a lone Higgs scenario we would not expect MUED to show a significant enhancement. If we see a suppression in the signal, we have to distinguish between LHT and the MSSM. Before we attempt to distinguish between the LHT and the MSSM based on large deviations in $B\sigma(gg \rightarrow h \rightarrow \gamma\gamma)$ alone, we first address what would happen if the LHC observes a Higgs boson with a deviation in $B\sigma(gg \rightarrow h \rightarrow \gamma\gamma)$ that is less than 30%.

B. Lone Higgs Scenario with a small deviation in $B\sigma(gg \rightarrow h \rightarrow \gamma\gamma)$

Suppose that the LHC finds a Higgs boson after 10 fb^{-1} whose $B\sigma(gg \rightarrow h \rightarrow \gamma\gamma)$ measurement deviates less than 30% from the expected SM value. Though we can not directly distinguish between the three new models of physics from the SM, our results may nonetheless be useful in devising further tests to distinguish the models, for example, with consistency checks. Broadly speaking, if the deviation of the signal is more than the eventual accuracy of 10%, then it may be worthwhile to pursue this deviation as both a lead for consistency checks and a bias for planning search strategies/signals that are more optimized to one particular model of new physics. That is, we are placing more confidence in the measurement than its uncertainty warrants, in the hope that subsequent measurements would improve the uncertainty without a great shift in the measured value.

For example, suppose that with 10 fb^{-1} of LHC data, the measured value of $B\sigma(gg \rightarrow h \rightarrow \gamma\gamma)$ shows a positive 20% deviation from the SM with a 30% uncertainty. While this is not a significant deviation from the SM and this deviation is likely to fluctuate (and

may even change its sign) with subsequent measurements, we can use this result to favor MUED over LHT and the MSSM, since neither of these models can give an enhancement in $B\sigma(gg \rightarrow h \rightarrow \gamma\gamma)$. As such a deviation corresponds to R^{-1} in the range of 800 to 900 GeV and the masses of the KK tops and KK gluons of about 1 TeV, we may use this deviation as a consistency check to rule out the MUED model if none of the heavy KK particle states is found, and seek other explanations for the enhancement in the Higgs signal.

As another example, suppose that we see a 20% suppression of the signal from the SM with 10 fb^{-1} of LHC data, we can then favor LHT and the MSSM over MUED, and optimize our search strategies in order to both find additional expected resonances in these models as well as devise tests that may distinguish these two models when we find these resonances. To be more concrete, let us also suppose that the Higgs mass is measured to be 125 GeV. Such Higgs mass is rather large in the scope of the MSSM, and is consistent with heavy s-tops, with perhaps significant mixing that evade direct discovery. If we favor the assumption Nature is supersymmetric, from Fig. 5, we see that a suppression of 20% in $B\sigma(gg \rightarrow h \rightarrow \gamma\gamma)$ corresponds to $M_A \sim 400 \text{ GeV}$. On the other hand, in the context of LHT, from the Fig. 11, we see that such deviation correspond to a rather low value of $f \sim 640 \text{ GeV}$. These pieces of information ($M_A \sim 400 \text{ GeV}$ or $f \sim 640 \text{ GeV}$) can then be used to devise search strategies that can differentiate MSSM from LHT.

C. Lone Higgs Scenario with a large deviation in $B\sigma(gg \rightarrow h \rightarrow \gamma\gamma)$

If the LHC finds a lone Higgs boson with $B\sigma(gg \rightarrow h \rightarrow \gamma\gamma)$ that deviates from the SM value by more than 30%, then the prospects are very exciting. First, in the case of an enhancement in the measurement, we can strongly disfavor all three models of new physics under considerations here, and seek alternative explanations for such an enhancement. Neither the MSSM nor the LHT can give a enhancement in $B\sigma(gg \rightarrow h \rightarrow \gamma\gamma)$ relative to the SM in a lone Higgs scenario, and this large enhancement can not be consistent with MUED because in that case some light KK resonances must be produced and detected at the LHC. (By definition, lone Higgs scenario requires that no other resonances being detected.)

In the case of a suppression, we would strongly favor MSSM and LHT over MUED and need to distinguish these two models based on the measured value of $B\sigma(gg \rightarrow h \rightarrow \gamma\gamma)$. As

a consistency check with both MSSM and LHT, the Higgs mass should be around $m_h \sim 125$ GeV to be consistent with both the MSSM (because the s-tops need to be heavy to evade discovery) and LHT (because of the large deviation in $B\sigma(gg \rightarrow h \rightarrow \gamma\gamma)$).

A possible first discriminating test between MSSM and LHT is the amount of deviation in $B\sigma(gg \rightarrow h \rightarrow \gamma\gamma)$. From Fig. 11, the LHT with $m_h \leq 130$ GeV can not give a suppression in $B\sigma(gg \rightarrow h \rightarrow \gamma\gamma)$ of more than 40%, while the MSSM with $10 \leq \tan\beta \leq 30$ can accommodate a suppression larger than 40% with $M_A \lesssim 300$ GeV as shown in Fig. 5. Therefore, a lone Higgs scenario with a suppression in $B\sigma(gg \rightarrow h \rightarrow \gamma\gamma)$ of more than 40% as compared to the SM can only be consistent with the MSSM. (As discussed in Section III A 1, if we impose minimal flavor violation, the 3σ uncertainties in the measurement of $\text{Br}(b \rightarrow s\gamma)$ imposes $M_A > 260$ GeV, and the suppression in $B\sigma(gg \rightarrow h \rightarrow \gamma\gamma)$ can not be more than 55% relative to the SM.) While the suppression between 30% and 40% in $B\sigma(gg \rightarrow h \rightarrow \gamma\gamma)$ relative to the SM prediction can be consistent with both the MSSM and the LHT, we propose possible tests that can distinguish these two models with more integrated luminosity in the next subsection.

D. Distinguishing different lone Higgs scenarios with more luminosity

Given a lone Higgs scenario with a measured suppression in $B\sigma(gg \rightarrow h \rightarrow \gamma\gamma)$ that is greater than 30% relative to the SM, we note in the previous subsection that

- if the suppression is greater than 40% relative to the SM, then MSSM is strongly favored, and,
- if the suppression in $B\sigma(gg \rightarrow h \rightarrow \gamma\gamma)$ relative to the SM is between 30% and 40%, then both the MSSM and the LHT are viable.

In this subsection, we discuss how we may distinguish the MSSM from the LHT when the suppression in $B\sigma(gg \rightarrow h \rightarrow \gamma\gamma)$ relative to the SM is between 30% and 40% with further LHC operations and seeking new resonances beyond 10 fb^{-1}

First we consider the case that the LHT is responsible for the observed suppression in $B\sigma(gg \rightarrow h \rightarrow \gamma\gamma)$ relative to the SM. In this case, a suppression of 30% or more in $B\sigma(gg \rightarrow h \rightarrow \gamma\gamma)$ relative to the SM prediction corresponds to $f < 560$ GeV. For $f = 560$

GeV, the viable range of κ_q is $1.25 < \kappa_q < 3$, and this viable range of κ_q becomes even smaller with smaller f . For example, with $f = 500$ GeV, the viable range of κ is $1.6 < \kappa_q < 2.2$. With more luminosity, the LHC should discover either Q_- and/or W_H because this viable range on κ disappears, and we no longer have a lone Higgs scenario. For example, with $f = 560$ GeV and 100 fb^{-1} of data, the LHC can discover W_H if $\kappa_q > 1.5$ (see Fig. 12(b)) and discover Q_- if $\kappa_q < 1.55$ (see Fig. 13). These two constraints of κ_q overlap, so at least one of W_H or Q_- should be discovered at 100 fb^{-1} , and if κ is between $1.5 < \kappa_q < 1.55$, then the LHC should discover both W_H and Q_- with 100 fb^{-1} .

If we assume that the MSSM is the model of new physics that underlies the observed lone Higgs scenario with a suppression in $B\sigma(gg \rightarrow h \rightarrow \gamma\gamma)$ between 30% and 40%, then Fig. 5 tells us that $290 \text{ GeV} \lesssim M_A \lesssim 350 \text{ GeV}$, and Fig. 9(c) gives us the viable region on $M_A - \tan\beta$ plane for a lone Higgs scenario. From Fig. 9(c), we also see, in some of the viable region, with higher luminosity the LHC has the potential to discover the heavy MSSM Higgs bosons H/A in the $H/A \rightarrow \bar{\tau}\tau$ mode. Unfortunately, unlike the case of the LHT, we are not guaranteed to discover additional resonances at the LHC with more luminosity. For example, with $\tan\beta = 10$, $M_A = 300$ GeV, and 10 fb^{-1} of LHC data, we have a lone Higgs scenario with a significant suppression in $B\sigma(gg \rightarrow h \rightarrow \gamma\gamma)$ compared to the SM prediction, but we are outside the LHC reach for the heavy MSSM bosons H/A even at 300 fb^{-1} of integrated luminosity.

We can also use the discovery of the heavy Higgs bosons H/A as a consistency check of MSSM for a lone Higgs scenario with a suppression in $B\sigma(gg \rightarrow h \rightarrow \gamma\gamma)$ of more than 40% relative to the SM. Suppose we have a lone Higgs scenario with a measurement of $B\sigma(gg \rightarrow h \rightarrow \gamma\gamma)$ that is suppressed by more than 40% relative to the SM. From Fig. 5, we see that such suppression corresponds to $M_A \lesssim 300(290)$ GeV if $\tan\beta = 10(20)$. In Fig. 15, we superimpose onto Fig. 9 with the contour that corresponds to having a 40% suppression in $B\sigma(gg \rightarrow h \rightarrow \gamma\gamma)$ relative to the SM and mark the viable region of parameter space. We see that in most of this parameter space, we have the potential to discover the heavy MSSM neutral Higgs boson H/A when the integrated luminosity is increased to 100 fb^{-1} if $\tan\beta$ is sufficiently large. And with 300 fb^{-1} of integrated luminosity, most of this parameter space is covered.

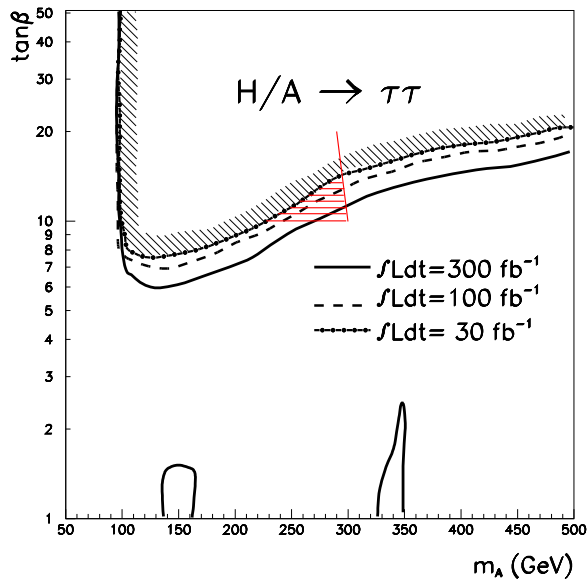


FIG. 15: We superimpose the discovery reach of H/A in the ATLAS TDR (Fig. 9(c)) with the upper bounds on M_A from a suppression of 40% in $B\sigma(gg \rightarrow h \rightarrow \gamma\gamma)$ (the negatively-sloped line). The hashed region below the intersection is the viable lone Higgs scenario region with a suppression in $B\sigma(gg \rightarrow h \rightarrow \gamma\gamma)$ of at least 40%. We assume $\tan\beta > 10$ throughout our analysis.

E. Other parameter-independent tests to distinguish the models

So far, we have attempted to use the lone Higgs scenario and a large deviation in the measurement of $B\sigma(gg \rightarrow h \rightarrow \gamma\gamma)$ to discriminate between MUED, LHT, and the MSSM. For some states in these models of new physics, such as the s-leptons of the MSSM, we can obtain viable lone Higgs scenarios by simply raising the masses of the new states large to evade discovery without affecting significantly the phenomenology of the discovered boson. It is possible that these states are discovered and identified only after 10 fb^{-1} of integrated luminosity, and these situations can certainly help us to further discriminate the models of new physics.

In this section we give some more tests of this type that can discriminate between MUED, LHT, and the MSSM, independent of the lone Higgs scenario. (Some of these tests have been stated in the literature.)

Since the MSSM is the most extensively studied model of new physics, and it has arguably the most complicated collider phenomenology of the three models that we study in this work,

we present tests that may separate LHT and MUED from the MSSM rather than identify MSSM directly.

1. Distinguishing MSSM and LHT with single- T_+ Production

In the MSSM, the cancellation of quadratic divergence introduces new states that differ in spin and must be pair-produced due to R -parity. In LHT, the new physics that modifies the properties of the Higgs boson come from the top-partners (T -parity even or odd) and the T -odd gauge bosons (W_H^\pm). The discovery potentials of the T -odd gauge bosons and top-partners were summarized in Section III B 2, and it was pointed out that, while the masses of the top-partners depend on additional inputs $\lambda_{1,2}$ (with the top quark mass as one constraint), the top-partners' contributions to $B\sigma(gg \rightarrow h \rightarrow \gamma\gamma)$ is independent of these parameters. Although we could raise the masses of both top-partners to evade LHC discovery at 10 fb^{-1} , naturalness arguments favor light top-partners and it is not implausible that we discover the top-partners after 10 fb^{-1} of operation. In naturalness arguments, the role of T_+ in LHT is played by the s-tops $\tilde{t}_{1,2}$ in the MSSM to cancel the quadratic divergences in the Higgs boson self energy, and, assuming we see new resonances related to an extended top-sector, we would like to distinguish T_+ and $\tilde{t}_{1,2}$.

One potential signature that can be used to distinguish LHT model from both the MSSM and MUED is the single-production of the T -even top-partner (T_+) [29]. The production mechanism of such signature is similar to the SM single-top production, with the top quark replaced by T_+ . As new colored states in both the MSSM and MUED must be pair produced, this can be used to distinguish the LHT from the MSSM and MUED. Furthermore, in the LHT the single-top production rate is suppressed as compared to the SM rate, and a precise measurement in single-top production rate can give us information about the top sector in LHT [53].

2. Distinguishing MSSM and MUED with single- H/A production

As stated earlier, the additional particle content in the MUED is very similar to that of the MSSM: the KK-modes are partners to the SM particle content in MUED just as the super-partners in the MSSM. Where as the gauginos obtain SUSY-breaking mass in the

MSSM, in MUED models, the n^{th} KK mode of the gauge bosons (A_μ^{th}) become massive through a ‘geometric’ Higgs mechanism: they eat linear combinations of (dominantly) the n^{th} fifth-dimensional component of the gauge bosons (A_5^{th}) and (sub-dominantly) the n^{th} mode of the Higgs boson H^{th} . At the first KK level, there are then four physical scalar bosons from the un-eaten combinations that are dominantly the first KK mode of the Higgs boson: $H^{\pm(1)}$, $\text{Re}[H^{0(1)}]$, and $\text{Im}[H^{0(1)}]$. Furthermore, in the limit that $R^{-1} \gg M_Z$ and if we assume no significant radiative corrections to the Higgs masses, these Higgs bosons will have similar masses with fractional degeneracies of the order $\mathcal{O}(m_h^2/R^{-2})$.

Effectively, the MUED also contains a two Higgs doublets just as the MSSM: the zeroth and first KK-level Higgs doublets. The Higgs sector in the first KK level of MUED models is similar to the MSSM heavy Higgs sector in many aspects:

- they both contain two electrically neutral (one CP -even and the other CP -odd) Higgs bosons, and a $Q_{em} = 1$ charged Higgs boson,
- these states are nearly degenerate: the fractional degeneracies in the masses are of the order $\mathcal{O}(M_Z^2/M_A^2)$ in the MSSM, and $\mathcal{O}(m_h^2/R^{-2})$ in MUED.

However, there is one crucial difference: the heavy Higgs bosons in MSSM are R -even and can be singly produced at the LHC, whereas these KK Higgs are K -odd and must be pair produced.

Unfortunately, as the LHC discovery potential for the singly-produced heavy Higgs bosons in the MSSM do not place stringent constraints on parameter space (this allows us to have a lone Higgs scenario with a large deviation in $B\sigma(gg \rightarrow h \rightarrow \gamma\gamma)$), discovering new physics through pair-produced Higgs bosons is much more difficult. Nevertheless, we point out this crucial difference in the Higgs sector in the MSSM and MUED since, as far as we know, it had not been explicitly stated in the literature. Furthermore, it could generate new signal event signatures outside the context of lone Higgs scenario.

V. CONCLUSIONS

In this work we attempt to distill traces of physics beyond the SM in the scenario that the LHC only discovers a Higgs boson after its initial years of operation with 10 fb^{-1} of data.

We focus on the scenario of light Higgs boson and used the signal $B\sigma(gg \rightarrow h \rightarrow \gamma\gamma)$ to distinguish between LHT, MUED, and the MSSM. For simplicity, in the MSSM we consider a limited lone Higgs scenario where the s-top soft masses are large enough that, in addition to evade direct discovery at the LHC, the s-top contributions to the gluon-gluon fusion and di-photon decay amplitudes decouple regardless of the value of A_t . Given the expected accuracies of the measurement of the Higgs-di-gluon and Higgs-di-photon couplings at this stage of operation of LHC, and the implications of lone Higgs scenario on the spectra of new physics, in MUED it is difficult to have significant deviations from the SM. In the cases of the LHT and the MSSM, however, it is possible to have a significant suppression in the signal while discovering a lone Higgs boson, and such lone Higgs scenario may give rise to a new resonance (H/A in the MSSM, and W_- or Q_- in the LHT) with more luminosity.

In the case where the measured deviation is very large, we offer tests that may potentially separate LHT from the MSSM even before a new resonance is discovered. In case where the deviation is small, our work may nevertheless be useful and we point out that the deviations can be used to bias a class of model from another, and as such can be useful in devising search strategies of the favored new physics.

Although we have only worked out detailed strategies for 10 fb^{-1} integrated luminosity in the case of lone Higgs scenario, similar kinds of considerations could also apply to various stages of LHC running. We hope to have demonstrated that even with the lone Higgs scenario, many insights can still be learned before the end of the LHC era.

Acknowledgments

This work is supported by the US National Science Foundation under grants PHY-0354226, PHY-0555545, and PHY-0354838. We thank Chuan-Ren Chen for carefully proof-reading this preprint. KH would like to thank R. Sekhar Chivukula, Elizabeth H. Simmons and Neil D. Christensen for stimulating discussions. We would also like to thank Michael Spira for his assistance with `hdecay`. We thank Qing-Hong Cao, Debajyoti Choudhury, and

Sven Heinemeyer for granting us permission to use the figures of their works.

- [1] A. Cho, *Science*, Vol. **315**. no. 5819, pp. 1657 - 1658
- [2] N. Arkani-Hamed, G. L. Kane, J. Thaler and L. T. Wang, *JHEP* **0608**, 070 (2006) [arXiv:hep-ph/0512190].
- [3] S. Mantry, M. J. Ramsey-Musolf and M. Trott, *Phys. Lett. B* **660**, 54 (2008) [arXiv:0707.3152 [hep-ph]].
- [4] S. Mantry, M. Trott and M. B. Wise, *Phys. Rev. D* **77**, 013006 (2008) [arXiv:0709.1505 [hep-ph]].
- [5] L. Randall, *JHEP* **0802**, 084 (2008) [arXiv:0711.4360 [hep-ph]].
- [6] “ATLAS detector and physics performance. Technical design report. Vol. 2,”
- [7] G. L. Bayatian *et al.* [CMS Collaboration], *J. Phys. G* **34**, 995 (2007).
- [8] P. M. Nadolsky *et al.*, arXiv:0802.0007 [hep-ph].
- [9] D. Zeppenfeld, R. Kinnunen, A. Nikitenko and E. Richter-Was, *Phys. Rev. D* **62**, 013009 (2000) [arXiv:hep-ph/0002036].
- [10] M. Duhrssen, S. Heinemeyer, H. Logan, D. Rainwater, G. Weiglein and D. Zeppenfeld, *Phys. Rev. D* **70**, 113009 (2004) [arXiv:hep-ph/0406323].
- [11] S. P. Martin, arXiv:hep-ph/9709356.
- [12] A. Djouadi, J. Kalinowski and M. Spira, *Comput. Phys. Commun.* **108**, 56 (1998) [arXiv:hep-ph/9704448].
- [13] S. Heinemeyer, W. Hollik and G. Weiglein, *Comput. Phys. Commun.* **124**, 76 (2000) [arXiv:hep-ph/9812320].
- [14] R. V. Harlander and M. Steinhauser, *JHEP* **0409**, 066 (2004) [arXiv:hep-ph/0409010].
- [15] F. del Aguila and L. Ametller, *Phys. Lett. B* **261**, 326 (1991).
- [16] H. Baer, C. h. Chen, F. Paige and X. Tata, *Phys. Rev. D* **49**, 3283 (1994) [arXiv:hep-ph/9311248].
- [17] H. Baer, C. h. Chen, F. Paige and X. Tata, *Phys. Rev. D* **52**, 2746 (1995) [arXiv:hep-ph/9503271].
- [18] S. Gennai, S. Heinemeyer, A. Kalinowski, R. Kinnunen, S. Lehti, A. Nikitenko and G. Weiglein,

- Eur. Phys. J. C **52**, 383 (2007) [arXiv:0704.0619 [hep-ph]].
- [19] E. Barberio *et al.* [Heavy Flavor Averaging Group (HFAG)], arXiv:hep-ex/0603003.
- [20] G. D’Ambrosio, G. F. Giudice, G. Isidori and A. Strumia, Nucl. Phys. B **645**, 155 (2002) [arXiv:hep-ph/0207036].
- [21] G. Degrossi, P. Gambino and P. Slavich, arXiv:0712.3265 [hep-ph].
- [22] B. C. Allanach, Comput. Phys. Commun. **143**, 305 (2002) [arXiv:hep-ph/0104145].
- [23] N. Arkani-Hamed, A. G. Cohen, E. Katz and A. E. Nelson, JHEP **0207**, 034 (2002) [arXiv:hep-ph/0206021].
- [24] H. C. Cheng and I. Low, JHEP **0309**, 051 (2003) [arXiv:hep-ph/0308199].
- [25] H. C. Cheng and I. Low, JHEP **0408**, 061 (2004) [arXiv:hep-ph/0405243].
- [26] I. Low, JHEP **0410**, 067 (2004) [arXiv:hep-ph/0409025].
- [27] N. Arkani-Hamed, A. G. Cohen, E. Katz, A. E. Nelson, T. Gregoire and J. G. Wacker, JHEP **0208**, 021 (2002) [arXiv:hep-ph/0206020].
- [28] For reviews of little Higgs models, see Refs. [29] and [30], and references therein.
- [29] T. Han, H. E. Logan, B. McElrath and L. T. Wang, Phys. Rev. D **67**, 095004 (2003) [arXiv:hep-ph/0301040].
- [30] M. Schmaltz and D. Tucker-Smith, Ann. Rev. Nucl. Part. Sci. **55**, 229 (2005) [arXiv:hep-ph/0502182].
- [31] J. Hubisz, P. Meade, A. Noble and M. Perelstein, JHEP **0601**, 135 (2006) [arXiv:hep-ph/0506042].
- [32] C. R. Chen, K. Tobe and C. P. Yuan, Phys. Lett. B **640**, 263 (2006) [arXiv:hep-ph/0602211].
- [33] Q. H. Cao and C. R. Chen, Phys. Rev. D **76**, 075007 (2007) [arXiv:0707.0877 [hep-ph]].
- [34] J. Hubisz and P. Meade, Phys. Rev. D **71**, 035016 (2005) [arXiv:hep-ph/0411264].
- [35] M. S. Carena, J. Hubisz, M. Perelstein and P. Verdier, Phys. Rev. D **75**, 091701 (2007) [arXiv:hep-ph/0610156].
- [36] D. Choudhury and D. K. Ghosh, JHEP **0708**, 084 (2007) [arXiv:hep-ph/0612299].
- [37] S. Matsumoto, M. M. Nojiri and D. Nomura, Phys. Rev. D **75**, 055006 (2007) [arXiv:hep-ph/0612249].
- [38] T. Appelquist, H. C. Cheng and B. A. Dobrescu, Phys. Rev. D **64**, 035002 (2001) [arXiv:hep-ph/0012100].

- [39] I. Antoniadis, Phys. Lett. B **246**, 377 (1990).
- [40] I. Antoniadis, N. Arkani-Hamed, S. Dimopoulos and G. R. Dvali, Phys. Lett. B **436**, 257 (1998) [arXiv:hep-ph/9804398].
- [41] N. Arkani-Hamed, S. Dimopoulos and G. R. Dvali, Phys. Lett. B **429**, 263 (1998) [arXiv:hep-ph/9803315].
- [42] N. Arkani-Hamed, S. Dimopoulos and G. R. Dvali, Phys. Rev. D **59**, 086004 (1999) [arXiv:hep-ph/9807344].
- [43] H. Georgi, A. K. Grant and G. Hailu, Phys. Lett. B **506**, 207 (2001) [arXiv:hep-ph/0012379].
- [44] H. C. Cheng, K. T. Matchev and M. Schmaltz, Phys. Rev. D **66**, 036005 (2002) [arXiv:hep-ph/0204342].
- [45] H. C. Cheng, J. L. Feng and K. T. Matchev, Phys. Rev. Lett. **89**, 211301 (2002) [arXiv:hep-ph/0207125].
- [46] G. Servant and T. M. P. Tait, Nucl. Phys. B **650**, 391 (2003) [arXiv:hep-ph/0206071].
- [47] G. Servant and T. M. P. Tait, New J. Phys. **4**, 99 (2002) [arXiv:hep-ph/0209262].
- [48] K. Kong and K. T. Matchev, JHEP **0601**, 038 (2006) [arXiv:hep-ph/0509119].
- [49] F. Burnell and G. D. Kribs, Phys. Rev. D **73**, 015001 (2006) [arXiv:hep-ph/0509118].
- [50] D. N. Spergel *et al.* [WMAP Collaboration], Astrophys. J. Suppl. **170**, 377 (2007) [arXiv:astro-ph/0603449].
- [51] D. Hooper and S. Profumo, Phys. Rept. **453**, 29 (2007) [arXiv:hep-ph/0701197].
- [52] F. J. Petriello, JHEP **0205**, 003 (2002) [arXiv:hep-ph/0204067].
- [53] Q. H. Cao, C. S. Li and C. P. Yuan, arXiv:hep-ph/0612243.